



Key Points:

- The 37 years, spring-time fast-ice thickness record in McMurdo Sound, Antarctica, has an interannual variability of up to 0.7 m and no trend
- Interannual variability in McMurdo Sound fast-ice thickness is not explained by monthly mean atmospheric heat fluxes alone
- Key influences on spring-time fast-ice thickness in McMurdo Sound are storm events, air temperature, and autumn to winter wind speed

Supporting Information:

Supporting Information may be found in the online version of this article.

Correspondence to:

M. E. Richter,
m.richter@uea.ac.uk

Citation:

Richter, M. E., Leonard, G. H., Smith, I. J., Langhorne, P. J., & Parry, M. (2024). The interannual variability of Antarctic fast-ice thickness in McMurdo Sound and connections to climate. *Journal of Geophysical Research: Oceans*, 129, e2023JC020134. <https://doi.org/10.1029/2023JC020134>

Received 13 JUN 2023

Accepted 11 NOV 2024

Author Contributions:

Conceptualization: Greg H. Leonard, Inga J. Smith, Pat J. Langhorne
Formal analysis: Maren Elisabeth Richter
Funding acquisition: Inga J. Smith, Pat J. Langhorne
Investigation: Maren Elisabeth Richter
Methodology: Maren Elisabeth Richter, Matthew Parry
Resources: Inga J. Smith
Software: Maren Elisabeth Richter
Supervision: Greg H. Leonard, Inga J. Smith, Pat J. Langhorne, Matthew Parry
Visualization: Maren Elisabeth Richter
Writing – original draft: Maren Elisabeth Richter

© 2024 The Author(s). This is an open access article under the terms of the Creative Commons Attribution-NonCommercial License, which permits use, distribution and reproduction in any medium, provided the original work is properly cited and is not used for commercial purposes.

The Interannual Variability of Antarctic Fast-Ice Thickness in McMurdo Sound and Connections to Climate

Maren Elisabeth Richter¹ , Greg H. Leonard² , Inga J. Smith¹ , Pat J. Langhorne¹ , and Matthew Parry³ 

¹Department of Physics, University of Otago, Dunedin, New Zealand, ²National School of Surveying, University of Otago, Dunedin, New Zealand, ³Department of Mathematics and Statistics, University of Otago, Dunedin, New Zealand

Abstract Land-fast sea-ice (fast ice) in McMurdo Sound grows through heat loss to the atmosphere and through heat loss to the ocean due to the presence of supercooled water. In this paper, we present a fast-ice thickness data set covering 1986–2022, providing a baseline of interannual variability in fast-ice thickness. Fast ice thicknesses are related to atmospheric and oceanic drivers on monthly and seasonal timescales to provide one of the longest timeseries of drivers of interannual fast-ice thickness variability from high-quality, in situ observations. We select a 14 km by 20 km area of level fast-ice over which atmospheric and oceanic drivers have negligible spatial variation, allowing us to resolve temporal variability in drivers and thickness. A statistical significance testing approach is adopted which only considers drivers that have a plausible physical mechanism to influence fast-ice thickness. We demonstrate that the fast-ice cover in McMurdo Sound is thicker in years when surface air temperature is colder, average (southerly) wind speed is higher, and there are fewer southerly storms. Nonetheless, we show that monthly averaged drivers have limitations and often do not produce strong correlations with thickness or fast-ice persistence. Consequently, most of the variability in fast-ice thickness cannot be explained by a single driver. No long-term trend in fast-ice thickness was found in eastern McMurdo Sound, thickness being influenced by a combination of drivers. Future event-based analyses, relating storms to fast-ice persistence, are needed. The present study provides a baseline against which these extreme events and long-term trends can be assessed.

Plain Language Summary Each winter the ocean in McMurdo Sound freezes to form sea ice. We present landfast sea-ice thickness measurements taken between 1986 and 2022, which we connect to properties of the atmosphere and the ocean. This provides a baseline of the variation in landfast sea-ice thickness between years. Our work highlights the atmosphere and ocean properties most likely to influence landfast sea-ice thickness in McMurdo Sound. In years when the air is colder, (southerly) wind speed is higher, and there are less southerly storms, the landfast sea ice is thicker. There remains a need for a future event-based analysis, especially around extreme storm events driving winter landfast sea-ice break up and persistence.

1. Introduction

Fast ice, defined as ice that has persisted for at least 15 days and is mechanically fastened to shoreline features, makes up $\sim 7\%$ of the total Antarctic sea-ice cover when it is at its minimum extent, and $\sim 3\%$ at its maximum (Fraser et al., 2021). Despite this small percentage, a recent review by Fraser et al. (2023) demonstrates that Antarctic fast ice is important because it provides buttressing to Antarctic continental ice, influences the size of polynyas and hence dense water formation, and it has a critical ecological function. There have been recent advances in detecting fast-ice extent (Fraser et al., 2012, 2021), but satellite observations of fast-ice thickness remain a challenge. This is due to difficulties in finding a mean sea level as reference for altimetry in fast ice (Kacimi & Kwok, 2020) as well as the unknown thickness and density of snow and the sub-ice platelet layer (Kurtz & Markus, 2012; Price et al., 2013, 2014; Yi et al., 2011).

The lack of fast-ice thickness information from satellite means that the only long-term measurements of fast-ice thickness in Antarctica come from sea-ice monitoring stations (SIMS) and manual thickness-tape measurements at a handful of locations (Arndt et al., 2020; Heil, 2006; Kim et al., 2018; Langhorne et al., 2015; Murphy et al., 1995, 2014). Most of these records do not indicate a significant trend in thickness over the observation periods (1950s–2000s, Heil (2006); 2010–2018, Arndt et al. (2020); 1902–2014, Langhorne et al. (2015)), although interannual variability can be high. Additionally, fast-ice properties may show cyclical signals on 2–20 years timescales (Murphy et al., 1995, 2014).

Writing – review & editing: Maren Elisabeth Richter, Greg H. Leonard, Inga J. Smith, Pat J. Langhorne

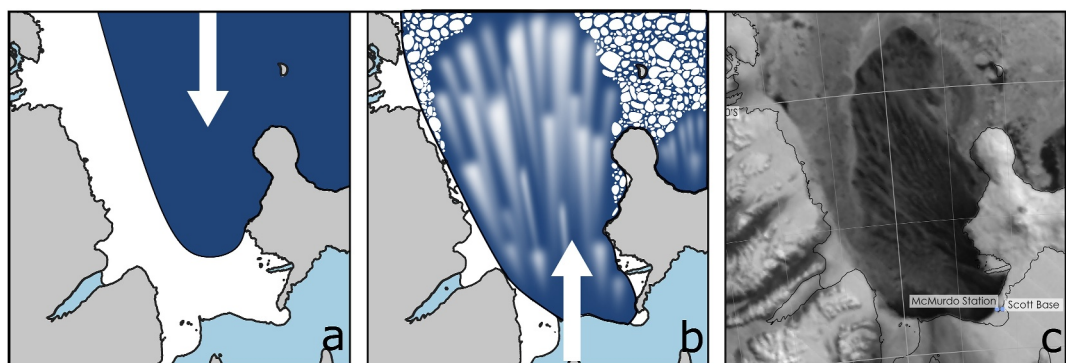


Figure 1. (a) + (b) Schematic of wind influencing fast-ice formation in McMurdo Sound, open water in dark blue, sea ice in white. Ice shelves and ice tongues (light blue), and land mask (gray) from the SCAR Antarctic Digital Database, accessed 2021. (a) Predominantly northerly winds (which can push existing pack-ice into the sound), or weak southerlies, lead to fast-ice freeze-up. Earlier fast-ice freeze up leads to thicker ice. (b) Strong southerly winds can break up the fast ice, opening up the McMurdo Sound polynya and exporting ice out of the sound. A later fast-ice formation leads to thinner ice. (c) MODIS SNPP VIIRS-Day-Night Band visible image of McMurdo Sound polynya opening on 15 June 2022. Illumination during polar night by the full moon. VIIRS image from <https://worldview.earthdata.nasa.gov>, processing courtesy of Jan Lieser.

Antarctic fast-ice thickness is influenced by heat transport to the atmosphere (Stefan, 1891) and ocean (Gough et al., 2012; Heil et al., 1996), as well as the timing of formation and breakout (Murphy et al., 1995). A higher atmospheric heat flux (due to lower surface air temperatures and/or higher surface wind speeds, e.g., Heil (2006)), increased heat loss to the ocean (in areas with upper ocean supercooling), and a longer growth season (e.g., Murphy et al. (1995)) all lead to thicker fast ice. The growth season is influenced by seasonal changes in ocean currents (and thus heat transport) and breakout events (Figure 1). Breakout events are in turn influenced by (a) timing, frequency and strength of off-shore storms during austral autumn and early winter (Leonard et al., 2021) which may break up and push thin fast ice away from the coastline; (b) ocean swell, which may cause fast-ice retreat from the seaward edge (e.g., Higashi et al., 1982); and (c) physical barriers such as icebergs preventing breakout (Brunt et al., 2006; Kim et al., 2018).

Beyond the fast-ice edge, studies have attempted to draw links between pack-ice extent and large scale atmospheric patterns such as El-Niño Southern-Oscillation (ENSO) (e.g., Baba & Renwick, 2017), Southern Annular Mode (SAM) (e.g., Baba & Renwick, 2017), Interdecadal Pacific Oscillation (IPO) (Chung et al., 2022; Meehl et al., 2016), Atlantic Multidecadal Oscillation (AMO) (Chung et al., 2022), or combinations thereof. The atmospheric patterns influence regional wind fields and the advection of heat, thus influencing the drift and melt/freeze cycle of pack ice. Surface air temperature in western Antarctica is influenced by the phases of SAM and ENSO (Clem et al., 2017). SAM and IPO influence the strength of the Amundsen Sea Low (Chung et al., 2022; Clem & Fogt, 2013; Meehl et al., 2016), which influences southerly winds in the western Ross Sea (Coggins & McDonald, 2015). These southerly winds in turn influence sea-ice production in the Ross Sea Polynya (Dale, 2020) and sea-ice extent (Meehl et al., 2016). The number of strong wind events in McMurdo Sound between 1979 and 2007 has been linked to ENSO 3.4 and SAM (Chenoli et al., 2012). ENSO and SAM have also been linked to the timing of the autumn ice-edge advance in the Ross Sea (in which McMurdo Sound is located) (Stammerjohn et al., 2008). Additional connections were found between sea-ice extent and autumn SAM, IPO, and AMO, amongst others (Yu et al., 2021). Hobbs et al. (2016) give a good overview of these interrelationships, confirming the lack of information on sea-ice thickness.

The aims of this paper are to (a) identify the key influences on the monthly averaged fast-ice thickness using a 37-year time series of fast-ice thickness in McMurdo Sound and local meteorological observations; (b) explore if interannual variability could be explained by wider influences such as climate modes. In order to identify drivers of temporal variability we need to select a fast-ice study area over which the influences of the atmosphere and ocean are approximately uniform at any given time.

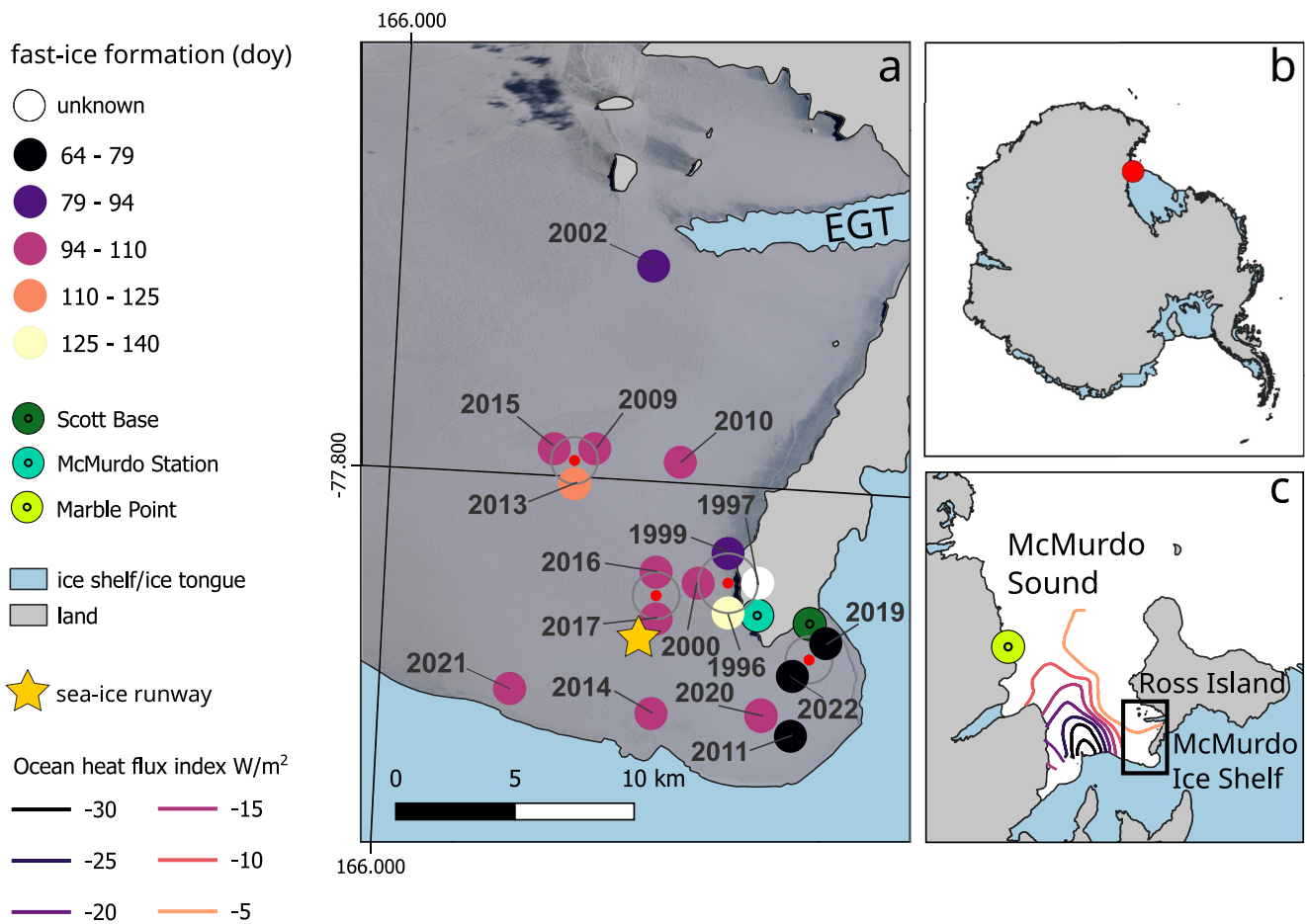


Figure 2. (a) Map of McMurdo Sound with position in Antarctica (b), and relative to Ross Island (c). Box in panel (c) marks zoomed in area displayed in panel (a). (a) Sea-ice monitoring stations locations as circles with year of deployment. The color of the circle corresponds to day of year the fast ice persisted (freeze-up date) at that location, see legend. The resolution of the freeze-up date is ~ 14 days, see Table 1, and the color grouping reflects that. If multiple deployments were at the same location, they are toggled around the central point (small red circle). EGT stands for the Erebus Glacier Tongue. The approximate location of the K2018 observations at the sea-ice runway is shown as a star, Scott Base as a dark green circle, and McMurdo Station as a cyan circle. Location of Marble Point in panel (c) as a light green circle. Background image in panel (a) pansharpened visible image from Landsat 8 taken on 15 October 2018. Image downloaded from USGS, courtesy of the U.S. Geological Survey. Panels (b) and (c) show a map of Antarctica (SCAR Antarctic Digital Database, accessed 2021), with land and grounded ice in gray, and ice shelves and glacier tongues in blue. Panel (c) shows contours of ocean heat flux index from Langhorne et al. (2015).

2. Background Information on McMurdo Sound Fast Ice

The fast ice of McMurdo Sound in the southwestern Ross Sea (Figure 2) has been critical as a platform for scientific operations in the region, yielding one of the longest fast-ice records. Observations stretch back to the British National Antarctic Expedition (1901–1904) in 1902 (Hodgson, 1907; Langhorne et al., 2015) with more frequent observations since the mid 1980s (Kim et al., 2018; Langhorne et al., 2015; Richter et al., 2022). Lying between Ross Island and the Victoria Land Coast, the southern limit of the sound is formed by the McMurdo Ice Shelf, the cavity of which is connected to the much larger Ross Ice Shelf cavity (Assmann, 2004). The surface circulation in McMurdo Sound is characterized by cold Ice Shelf Water (ISW) flowing north from underneath the McMurdo Ice Shelf in the western sound (Robinson et al., 2014). During winter, this surface ISW outflow spreads to most of the sound (Leonard et al., 2006; Mahoney et al., 2011; Robinson et al., 2014). The ISW is often in-situ supercooled (it is colder than its in situ freezing point temperature (Jacobs, 2004; Jacobs et al., 1985; Leonard et al., 2006, 2011; Lewis & Perkin, 1985; Mahoney et al., 2011; Robinson et al., 2014), allowing the formation of a sub-ice platelet layer (SIPL; e.g., Hoppmann et al. (2020)) underneath the sea ice. If the sea ice grows into the interstices of the friable and porous SIPL, incorporated platelet ice is formed. This causes the sea ice in McMurdo Sound to grow thicker than through atmospheric heat flux alone (Gough et al., 2012; Hellmer, 2004; Hoppmann et al., 2020; Purdie et al., 2006). The proximity of the ice shelves means that there has been no statistically

significant change in SIPL thickness and winter near-surface ocean temperature in McMurdo Sound since the earliest observations in 1902 and 1922, respectively (Langhorne et al., 2015). We thus have the unique opportunity to study a relatively stable environment without strong long-term change, over a period of time that is long enough to identify interannual variability and its drivers.

Kim et al. (2018) have studied fast-ice thickness and temperature from repeat manual measurements at the McMurdo Sound sea-ice runway as well as fast-ice extent and duration from satellite data. They have found that fast-ice extent and duration are correlated with local wind, and that summer fast-ice retreat dates are not significantly correlated to fast-ice thickness. Winter fast-ice breakout events in McMurdo Sound are mainly wind driven (Crocker & Wadhams, 1989; Kim et al., 2018; Leonard et al., 2021).

From 2001 to 2011 large icebergs blocked the mouth of McMurdo Sound, causing anomalous sea-ice and ocean conditions (Brunt et al., 2006; Kim et al., 2018; Robinson & Williams, 2012). Multi-year fast ice covered large parts of the sound, leading to an unusually large extent and thickness (Brunt et al., 2006; Kim et al., 2018) and to an average age close to 24 months over the time period 2000–2018 (Fraser et al., 2021). However, multi-year fast ice in McMurdo Sound is the exception rather than the norm for periods not influenced by icebergs (Heine, 1963; Kim et al., 2018; Langhorne et al., 2015; Prebble, 1968; Richter et al., 2022).

The presence of fast ice in the sound precludes satellite sea surface temperature (SST) observations, and this lack of observations makes reanalysis products for the ocean poorly constrained. Instead, we use two different proxies for ocean heat flux which are described below. Unfortunately, oceanographic records in McMurdo Sound are neither long enough nor have the temporal resolution to compare to our fast-ice observations. Consequently we focus on the role of atmospheric drivers (observations and climate modes) that have been shown to have an influence on sea-ice conditions in the wider Ross Sea.

3. Methods

Fast-ice thickness at the end of spring is the sum of two components: (a) the thickness at the start of observations, after fast ice has stabilized; and (b) the time integral of the rate of change of ice thickness since the start of observations. Initial thickness (a) is strongly dependent upon the date at which the fast ice cover becomes established in early winter. The integral of ice growth rate (b) depends upon the heat exchange with the atmosphere and ocean through winter and spring. Guided by this synopsis, we seek information on potential drivers of fast ice thickness. We follow the recommendations of Gelman and Hill (2007) to adopt a statistical significance testing approach that is informed by clear scientific reasoning. For example, we have only considered drivers having a plausible physical mechanism to influence fast-ice thickness.

We have selected a 14 km by 20 km area of level fast-ice over which ocean heat flux index is relatively uniform (Figure 2c and Langhorne et al. (2015)) and atmospheric drivers are unlikely to vary spatially. Within this area we utilize two fast ice thickness data sets: temperature records from SIMS deployed between 1996 and 2022, and thicknesses reported in Kim et al. (2018), as detailed below.

3.1. The Sea Ice Monitoring Station and Data of Kim et al. (2018)

Each University of Otago sea-ice monitoring station (SIMS) deployed in McMurdo Sound consisted of a 2–3 m long string of thermistors which were used to measure the temperature of the sea ice and underlying ocean at 5–10 cm vertical intervals every 10–15 min (Richter et al., 2022). A SIMS has been deployed most years since 1996 (Trodahl et al., 2000) within a 14 km by 20 km area (see Figure 2). We used the method described in Gough et al. (2012), with some manual adjustment, to identify the ice–ocean boundary from temperature measurements collected between 1996 and 2022 (Richter et al., 2022). This was combined with tape measurements through drill holes, where available. Uncertainties in sea-ice thickness, derived with the methods detailed in Richter et al. (2022), were 1 ± 2 cm, and thus an order of magnitude lower than the interannual variability in McMurdo Sound.

The location of the SIMS within the study area (circles in Figure 2a) was driven by varying factors in each year. Deployment in the years 2011, 2019, 2020, and 2022 was mainly the result of the presence of tidal cracks, rough fast ice or thinner ice (2022) in the main sound, making access to fast ice farther from Scott Base difficult. The location close to the Erebus Glacier Tongue (2002 deployment) was driven by other scientific considerations not associated

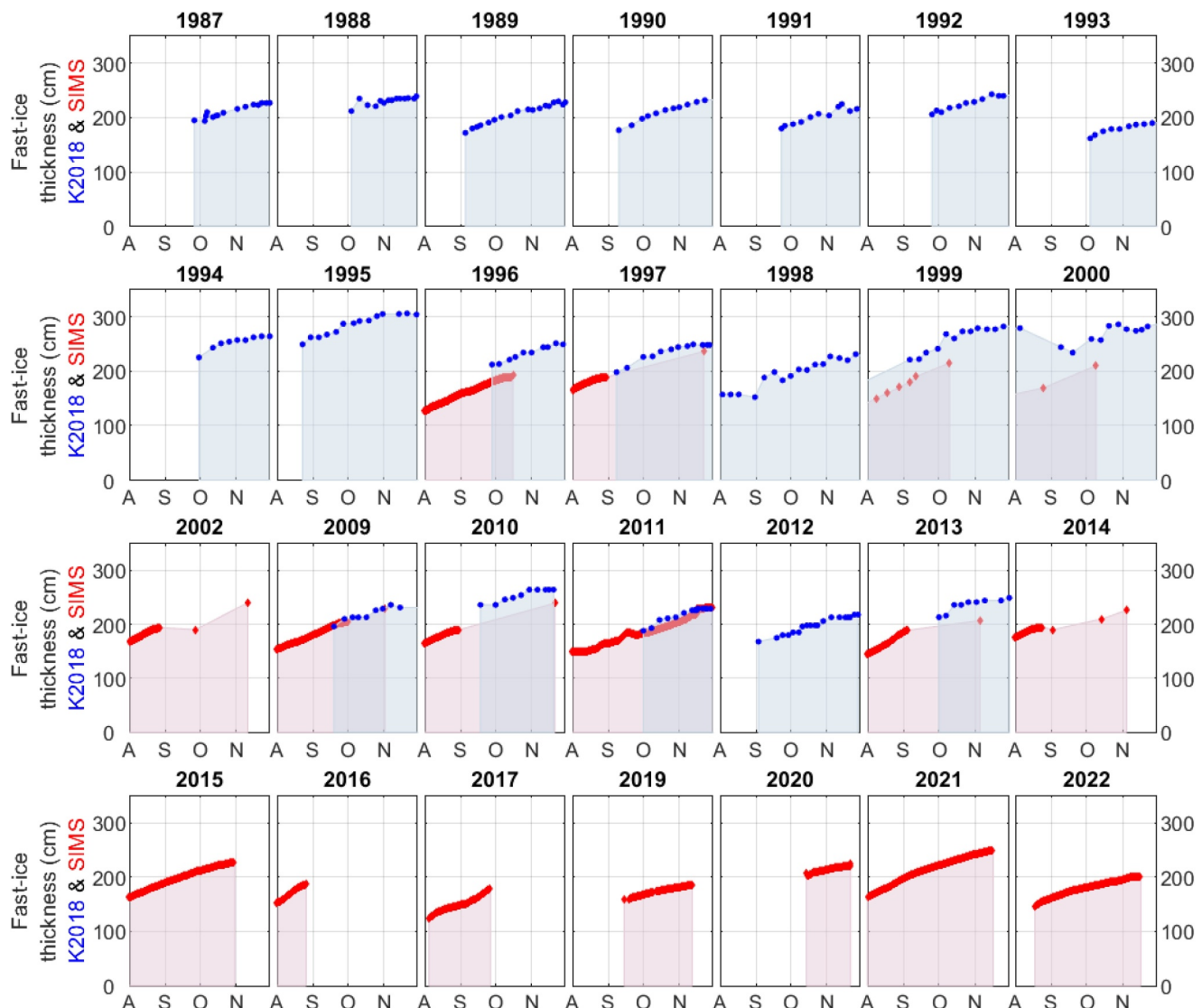


Figure 3. Time series of first-year fast-ice thicknesses in McMurdo Sound measured with a sea-ice monitoring station (sea-ice monitoring stations, locations in Figure 2) and with manual drill hole measurements, and at the sea ice runway (Kim et al., 2018; location in Figure 2). Vertical grid lines are on the 15th of the month for August (A), September (S), October (O), and November (N). Years for which we do not have first-year fast-ice thicknesses are not included.

with the SIMS. During the iceberg years (2001–2011) the need to find a location with first-year sea-ice was the primary concern. Locations in all other years were chosen to best reflect level first-year fast ice in the eastern sound.

To extend the record of the SIMS, we include manual thickness measurements at the US operated sea-ice runway (Kim et al., 2018, K2018 henceforth; and J. Scanniello, personal communication, April 2024). Fast-ice thicknesses from K2018 (the star in Figure 2a), are shown in Figure 3. Every date/thickness pair in the data published by Kim et al. (2018) is an average of 20–40 measurements along the length of the runway (J. Scanniello, personal communication, April 2024). The runway was established almost every year between 1985 and 2013, and a snow plough kept it snow free from the time of the first thickness observations in August/September. The lack of snow increases heat loss to the atmosphere, and thus growth rate and thickness of the fast-ice. We were interested in interannual variability, and the removal of snow in years with low ambient snow cover will have less of an effect on fast-ice growth than in years with a high snow cover. However, sensitivity tests, given below, show that the removal of the snow cover from September onwards, when the fast ice is more than 1 m thick at the Kim et al. (2018) site, does not unduly influence interannual variability in thickness. Since negative freeboards and snow-ice formation

are rare in McMurdo Sound (Dempsey et al., 2010; Gow et al., 1998; Price et al., 2014) snow on sea ice in McMurdo Sound in late winter/spring will only modulate ice–air heat fluxes and thus fast-ice growth rate.

Data collected at the SIMS sites and the sea-ice runway generally spanned August through November (Figure 3) as measurements relied on a well-established fast-ice cover that was thick enough to support vehicles. There were insufficient observations during earlier and later months to produce reliable information on interannual variability. We used monthly fast-ice thickness data, as the frequency of the observations did not allow for a higher resolution. The climate modes were also provided as monthly averages. This naturally limited us to monthly or seasonally averaged effects of drivers, and precluded any investigation of synoptic scale effects. However, the benefit was the much extended time series by including the K2018 data and information from manual fast-ice thickness measurements at the SIMS sites. We extracted monthly sea-ice thickness from the available observations detailed in Kim et al. (2018) and Richter et al. (2022) for August–November, by linearly interpolating thicknesses to yield mid-month values. The number of monthly averages thus obtained over all years is shown in Table 2. To create a time series 1986–2022, we adjusted the means of the monthly thickness of the K2018 data so that they matched the SIMS data. This ensured a time series that reflects the interannual variability in fast-ice thickness. To test for the possible error with this approach we used a simple 1-D sea ice growth model (Bitz & Lipscomb, 1999) with a setup following Smith et al. (2015). We made repeat runs with and without snow cover for the years 1999 and 2009, which are years with comprehensive supporting data, for example, sea-ice cores taken and snow depth measurements made at other McMurdo Sound sites in addition to the SIMS site, see Smith et al. (2001, 2015). Freeze up dates of the fast ice were taken as three sensitivity values: the earliest, most likely, and latest possible date from our analysis of satellite observations, with separate model runs for each of these dates. Ocean heat flux changed from 0 W m^{-2} to -13 W m^{-2} on day 197 in 1999, the day the sea-ice structure changed from columnar to incorporated platelet ice. For 2009, this change in ocean heat flux was chosen to occur on day 106, the day that made the modeled growth rate most closely resemble the measured growth rate for realistic freeze in, snow, and ocean heat flux values. Snow cover was obtained using NASA MERRA 0.25° reanalysis-derived snow cover (Rienecker et al., 2011) scaled to result in 6.5 and 15 cm snow cover for 10 October 1999 and 1 October 2009, respectively. This matches dates of measured snow depths during fieldwork. The mean difference in fast-ice thickness between the runs for the months August (which was 0.2 m in 1999 and 2009) and November (which were 0.3 m in 1999 and 0.1 m in 2009) was similar to the mean difference of 0.24 m between the K2018 and SIMS data for the same time period.

Our record of sea-ice thicknesses overlapped the time period in which large icebergs influenced the sea ice in McMurdo Sound. To avoid biases, we disregarded all years with multi-year ice at the site of measurement.

At the SIMS sites, the standard deviation of fast-ice thickness was $\sim 20 \text{ cm}$, with monthly average thicknesses increasing from $167 \pm 20 \text{ cm}$ to $223 \pm 20 \text{ cm}$ between August and November. At the K2018 site, the standard deviation of fast-ice thickness was higher, with monthly average thicknesses ranging from $208 \pm 60 \text{ cm}$ to $240 \pm 30 \text{ cm}$ for August and November, respectively. After the adjustment of the means of the K2018 thickness distribution, monthly average fast-ice thicknesses ranged from $164 \pm 20 \text{ cm}$ to $219 \pm 26 \text{ cm}$ for August and November, respectively. There was no inter-annual trend in fast-ice thickness.

3.2. Date of Fast-Ice Formation

Dates of fast-ice formation (Freeze-up dates) were extracted from the Fraser and Massom (2020) data set for years 2000–2018, and are shown in Table 1. Resolution was improved, and the time series extended, with synthetic aperture radar images available through ASF Vertex (<https://search.asf.alaska.edu/>) and ESA EO CAT (<https://eocat.esa.int/>).

3.3. Ocean Heat Flux

To investigate the contribution of ice grown through ocean heat loss to fast-ice thickness, we utilized two measures of ocean heat flux. We use a mean, late-winter, ocean heat flux index calculated from approximately 100 observations of incorporated platelet ice and sub-ice platelet layer thickness in McMurdo Sound collected between 1966 and 2014 (Langhorne et al., 2015). The ocean heat flux index is found by assuming that all the ice of the sub-ice platelet layer, and a fraction of the incorporated platelet ice, has been formed due to heat loss to the water column. This ocean heat flux index does not resolve interannual variability, but does provide the spatial pattern of ocean heat flux over the entire McMurdo Sound (see Figure 2c). To resolve interannual variability, ocean heat flux

Table 1*Date of Fast-Ice Formation From Satellite Retrievals for Years in Which There Are Fast-Ice Thickness Observations*

Year	Date of freeze up SIMS (doy)	Days to next image confirming freeze-up	Source	Date of freeze up K2018 (doy)	Days to next image confirming freeze-up	Source
1996	12.06. (164)	48	ESA	12.06. (164)	48	ESA
1997				03.05. (123)	30	
1999	27.3. (86)	9	ESA			
2000	15.4. (106)	14		15.4. (106)	14	
2002	1.4. (91)	14				
2009	27.4. (117)	14	Gough (2012)			
2010	12.4. (102)	11	ESA			
2011	14.3. (73)	18	ESA	01.05. (121)	15	
2012	29.6. (181)	14		29.06. (181)	14	
2013	16.4. (106)	14		16.04. (106)	14	
2014	16.4. (106)	14				
2015	14.4. (104)	12				
2016	18.4. (109)	14				
2017	16.4. (106)	15				
2019	18.3. (77)	12	ESA			
2020	17.4. (108)	12	ESA			
2021	12.4. (102)	12	ESA			
2022	14.3. (73)	12	ESA			

Note. Day of year (doy) of freeze up in brackets. If no additional source is given, dates are retrieved from the Fraser and Massom (2020) data set. See Figure 2 for a visual representation of the data presented here. Sources marked as ESA were viewed via the ESA EO CAT service <https://eocat.esa.int/>.

was calculated from measurements of fast-ice temperature gradients following Smith et al. (2012). Here, $F_w = F_c + F_l + F_s$ with F_w the ocean heat flux, F_l the latent heat flux, F_c the conductive heat flux, and F_s the sensible heat flux. The conductive heat flux is calculated from the vertical temperature gradient in the ice, 30–10 cm above the ice-ocean interface and assuming a thermal conductivity of $2.15 \text{ W m}^{-1} \text{ K}^{-1}$ (Pringle et al., 2006, 2007). The latent heat flux is calculated from the fast-ice growth rate assuming a sea-ice density of 920 kg m^{-3} (Pringle et al., 2007) and a latent heat of 352 kJ kg^{-1} (Ono, 1967). The sensible heat flux is assumed to be negligible. We disregard ocean heat flux values taken from the first 2 weeks after deployment to avoid the deployment of the probe influencing the results. The final thermistor to freeze in also routinely causes biases and is disregarded. Average annual winter values are given in Table S3 in Supporting Information S1 and shown in Figures 5 and 6c.

3.4. The Meteorological and Climate Mode Data

Atmospheric variables were measured at Scott Base, McMurdo Station, and Marble Point. Coverage of the meteorological data used in this study is shown in Table S2 in Supporting Information S1 and availability of the atmospheric data is given in the Open Research section. We refer to “strong southerly winds” in McMurdo Sound and not to “katabatic winds.” Katabatic winds are defined as flowing down a slope (Glossary of the American Meteorological Society https://glossary.ametsoc.org/wiki/Katabatic_wind) and their forcing has a slope driven component (Ball, 1956). The McMurdo Ice Shelf is virtually flat so that any winds blowing from the ice shelf into the sound cannot be katabatic winds by definition. More information on this can be found in Dale (2020).

Although climate modes have been shown to influence Antarctic sea-ice extent (see Section 1), so far no studies exist linking these to fast-ice

Table 2*Number of Monthly Averaged Sea-Ice Thickness Observations for Each Data Set Included Here*

	Number of observations			
	August	September	October	November
SIMS	10	11	11	6
K2018	3 ^a	7	17	17
All	12	16	23	18

Note. “All” means all years available, with some overlap between sea-ice monitoring stations and K2018 data. ^aNot used in our regressions due to low number of data points.

thickness in Antarctica. We used annual, seasonal, and monthly averages of the ENSO 3.4 index; the SAM index derived from station pressure data (Marshall, 2003); the AMO (Enfield et al., 2001); and the IPO (Henley et al., 2015). To capture the effect of ENSO and SAM together we investigated the influence of a combined ENSO/SAM index on fast-ice thickness. This index was defined here as the normalized ENSO index multiplied with the normalized SAM (SAMxENSO henceforth), and has been shown to influence sea-ice extent (e.g., Stammerjohn et al., 2008). Data availability is given in the Open Research section of this manuscript.

Because many climate indices show a seasonal cycle in their values, we used anomalies of the monthly (or seasonal) mean values for our analysis. This ensures, that for example, June values were compared to what is “normal” for June.

Meteorological and climate mode data were processed by calculating annual, seasonal, and monthly means (excluding the year studied), and then calculating the annual, seasonal, and monthly anomalies for every year. We examined the components of the wind (U and V) and directionless wind speed separately. The V component of the wind is positive for wind from the south (southerly or meridional wind); the U component of the wind is positive for wind from the west (westerly or zonal wind).

The modified storm index (MSI) was calculated from negative pressure, and positive temperature anomalies after Brunt et al. (2006); Leonard et al. (2021), and is a measure of the storminess of the southerly wind. Low air pressure and warm near-surface air temperature are typical for strong southerly winds in McMurdo Sound during winter (Chenoli et al., 2012; Coggins et al., 2013). High wind speeds cause the positive temperature anomaly through vertical mixing between the cold surface inversion layer and the warmer atmosphere above (Cassano et al., 2016).

3.5. Relationships Between Sea-Ice Thickness and Potential Drivers

We varied the SIMS thicknesses within their measurement uncertainty (Richter et al., 2022) to produce three thickness timeseries: the most likely thickness and two alternate results achieved by modifying the method of determining thickness. The SIMS data were then combined with the K2018 data to extend the data set to cover 1986–2022. We calculated the linear regression between nearly 3,000 combinations of the monthly fast-ice thicknesses and monthly, seasonal, and annual averages of the drivers. We report the sign of the slope of the linear regression (positive is correlated and negative is anti-correlated), r^2 , and p -value. r^2 is the correlation coefficient of the fit, and gives the percentage of variance in the signal explained by the driver. The p -value gives the likelihood percentage that the slope of the regression is zero, and was calculated with an F -test in ANOVA. The small variations in thickness to account for systematic errors allowed us to test the robustness of the correlation and we report only those correlations that were significant (p -value <0.05) for three variations of the time series and which have an r^2 value over 0.2.

4. Results

4.1. Influence of Location Within the Study Site: Ocean Heat Flux, Freeze Up Date, and Thickness

We begin by checking that spatial variations within our fast-ice study area do not confound our ability to resolve temporal variations.

We did not find a strong relationship between location within the study area and freeze-up date (correlation not shown, but see Figure 2 for a visual representation). In addition, the spread of freeze-up dates for the data of Kim et al. (2018) is similar to that of the SIMS locations (Table 1). Nor were there significant correlations between freeze-up date and thickness for both the K2018 and the SIMS data (not shown).

Ocean heat flux is known to be strongly location-dependent over McMurdo Sound (see Figure 2c and e.g., Hughes (2013); Langhorne et al. (2015)), and it is necessary to establish that this does not influence our conclusions for the much smaller area of the study site. Since we are limited in our knowledge of the ocean influencing the fast ice, we examined three variables associated with ocean conditions.

First consider (i) a spatially varying, but temporally averaged, ocean heat flux index from Langhorne et al. (2015) (Figure 6). We have evidence that this spatial pattern does not vary greatly between years (e.g., Brett et al., 2020; Dempsey et al., 2010; Haas et al., 2021; Langhorne et al., 2015). The Langhorne et al. (2015) data set is thus suitable to study the effect of the spatial variability of ocean heat flux in McMurdo Sound on our thickness

Table 3

r^2 and p -Values for Correlations Between Sea-Ice Thickness Measured by the Sea-Ice Monitoring Stations in Different Months and Depth of Columnar to Incorporated Platelet-Ice Transition ($c2p$) in Co-Located Ice Cores, and the Ocean Heat Flux Index From Langhorne et al. (2015)

	August		September		October		November	
	r^2	p	r^2	p	r^2	p	r^2	p
$c2p$ transition	0.01	0.807	0.32	0.071	0.45	0.023	0.67	0.047
Ocean heat flux index	0.05	0.455	0.00	0.891	0.00	0.918	0.08	0.490

Note. The sign reported with the r^2 value is the sign of the slope of the regression.

observations. We found that ocean heat flux index at the measurement locations was not significantly correlated with fast-ice thickness (Table 3).

Second (ii), as detailed in Methods, we calculated residual heat flux to test for interannual variability in ocean heat flux not resolved in Langhorne et al. (2015). This is interpreted to be the ocean heat flux, calculated from vertical temperature gradients in the sea ice following (Smith et al., 2012). Average winter values are given in Table S3 in Supporting Information S1 and shown in Figures 5 and 6c. As with the ocean heat flux index from Langhorne et al. (2015), there is no significant correlation with fast-ice thickness. We also examine conductive and latent heat fluxes, calculated by the same method, and again find no significant correlations with fast-ice thickness.

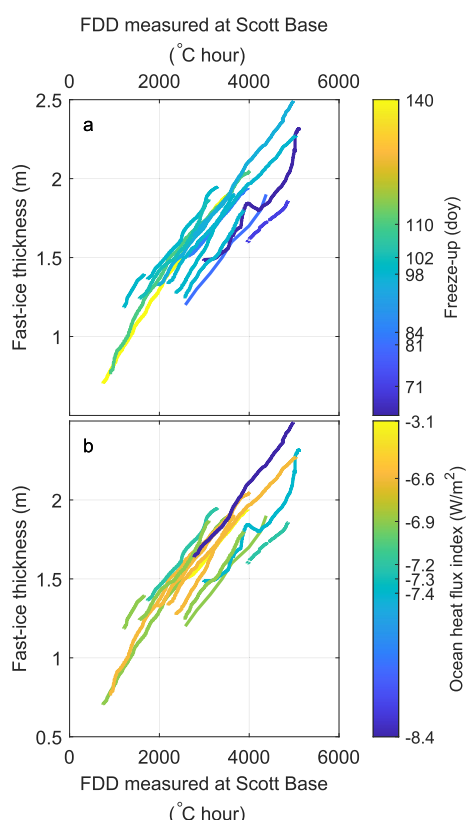


Figure 4. Inter-annual fast-ice thickness versus daily FDD measured at Scott Base since the date of fast-ice freeze-up for each year. Colors are for (a) day of fast-ice formation; and (b) multi-year ocean heat flux index at site from Langhorne et al. (2015). Values for individual years can be found in Table S3 in Supporting Information S1.

Finally, we examine (iii) the depth of the columnar to incorporated platelet ice transition, which marks the time at which the growth through heat loss to the ocean becomes large enough, compared to growth through heat loss to the atmosphere, that an SIPL forms. The SIPL is progressively incorporated into the sea ice through continued heat loss to the atmosphere. The years for which ice fabric information exists at the SIMS sites are shown in Table S1 in Supporting Information S1. We found no significant correlation between sea-ice thickness measured at the SIMS and the depth of the columnar to incorporated platelet-ice transition from ice cores taken close to the site of the thickness measurements (Table 3).

We describe sea-ice growth in terms of freezing degree days (FDD) since the date of fast-ice formation (e.g., Maykut, 1986) using daily Scott Base data for the years in which we have freeze up dates (Figure 4). We explore the dependence upon (a) the day of fast-ice freeze-up; and (b) the ocean heat flux index averaged over multiple years from Langhorne et al. (2015) for the location of the SIMS deployment (see Figure 2).

We can see that variation on sub-monthly scales is generally low (Figure 4), increasing our confidence that the use of monthly fast-ice thickness did not oversimplify the results.

Figure 4 also shows that FDD since freeze-up alone could not explain the annual variation in fast-ice thickness, nor was the remaining difference explained by spatial variability in the ocean heat flux index (Figures 4b and 5) over the range of measurement locations in the eastern sound (Figure 2a). The date of fast-ice persistence (freeze-up date) did seem to have some influence (Figure 4a), but not in the way one would expect, with years with a late freeze-up date and low FDD since freeze up, having greater fast-ice thickness than years with the same FDD since freeze up, but an earlier fast-ice formation.

Based on the arguments in this section, we proceed with confidence that our study site may be regarded as one over which the potential drivers of fast ice thickness are relatively uniform at any given time.

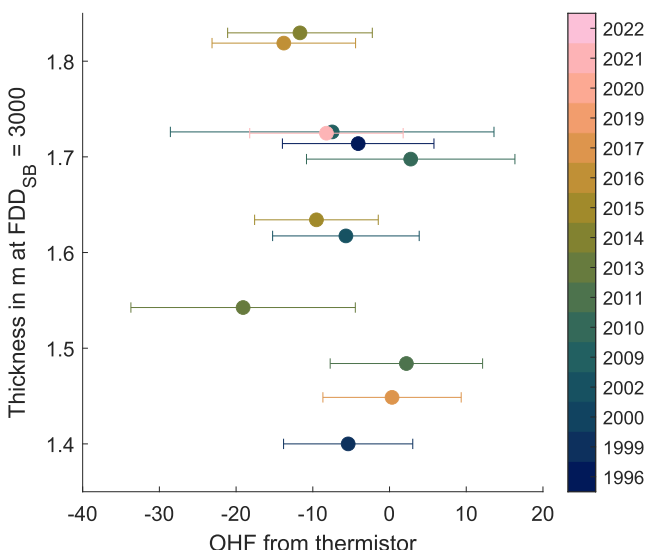


Figure 5. Thickness at $FDD = 3,000$ against ocean heat flux (Figure 6) at the location of the measurement. FDD as measured at Scott Base.

4.2. Correlations Between Fast-Ice Thickness and Meteorological Observations

Although highly variable, there were no obvious trends in fast-ice thickness anomaly (yearly thickness minus the average over all years), or drivers, as shown in Figure 6. This points to the likelihood that dominant drivers of fast-ice thickness may be monthly to seasonal rather than longer term and related to the changing climate. Thus, we focused on monthly and seasonal linear regressions of drivers and thicknesses, including lags of up to 5 months. We also examined trends in drivers to get an understanding of possible changes in the environment over the course of our observations, and this information is included in Figure S1 in Supporting Information S1.

As expected, the variables with the most significant correlations over the entire time series were $Tair$ and FDD , with lower air temperatures and higher number of FDD correlated to thicker ice (Figure 7). Significant anti-correlations with thickness were mainly found for March through August air temperatures. For the SIMS, calculating FDD since freeze up did not improve the correlation with thickness compared to FDD since start of the year. For the combined data set, however, FDD since start of the year was mostly not correlated to thickness whereas FDD since freeze up was. There were no significant correlations between FDD and the K2018 data, and very few between air temperature and the K2018 data.

Higher pressure in winter (JJA) was correlated with thicker ice in October and November. The correlations between thickness and pressure were significant for the combined and the K2018 data but not for the SIMS data.

Good quality wind speed data (no long gaps and no unphysical data) over the entire 1985–2022 range were only available for McMurdo Station and Marble Point. Good quality wind data from Scott Base was only available for 1999–2022. Stronger southerly winds (V-wind) from July to November were almost always correlated with thicker ice for the combined and/or K2018 thickness data sets. These correlations were stronger and more significant for October and November thicknesses. We found no significant correlations with zonal wind.

Correlations between thickness and wind speed were very similar to correlations between thickness and the southerly wind component (i.e., stronger winds correlated with thicker ice). The exception to this was the anti-correlation of Scott Base (Figure 7) and McMurdo Station (Figure S3 in Supporting Information S1) wind speeds in June with October fast-ice thickness measured by the SIMS. Scott Base wind speeds in June and McMurdo Station wind speeds in winter (JJA) were also anti-correlated with November fast-ice thickness from the SIMS.

Thickness measured between August and November was anti-correlated with May through August MSI and October thickness was positively correlated with spring (SON) and October MSI. There were no significant correlations between K2018 fast-ice thickness and MSI. All of these correlations will be discussed in detail in Section 5.

4.3. Correlations Between Freeze-Up Dates and MSI

From an operational viewpoint, it is interesting to understand how the storm index is related to the date when a location in McMurdo Sound forms a stable fast-ice cover. We calculated correlations for the years for which we have this information (see Table 1) and found positive correlations between freeze-up date and autumn (MAM) and April MSI (stronger storminess led to delayed fast-ice formation) and a negative correlation between freeze-up date and winter (JJA) MSI. Except for April MSI, most of these correlations were weak.

4.4. Correlations Between Fast-Ice Thickness and Climate Modes

Climate modes influence sea ice on much larger temporal and spatial scales than medium range (monthly or seasonal) weather, and the pathways through which they influence sea ice are not always straight forward. We examined those patterns that have been associated with Antarctic sea ice previously, as discussed above.

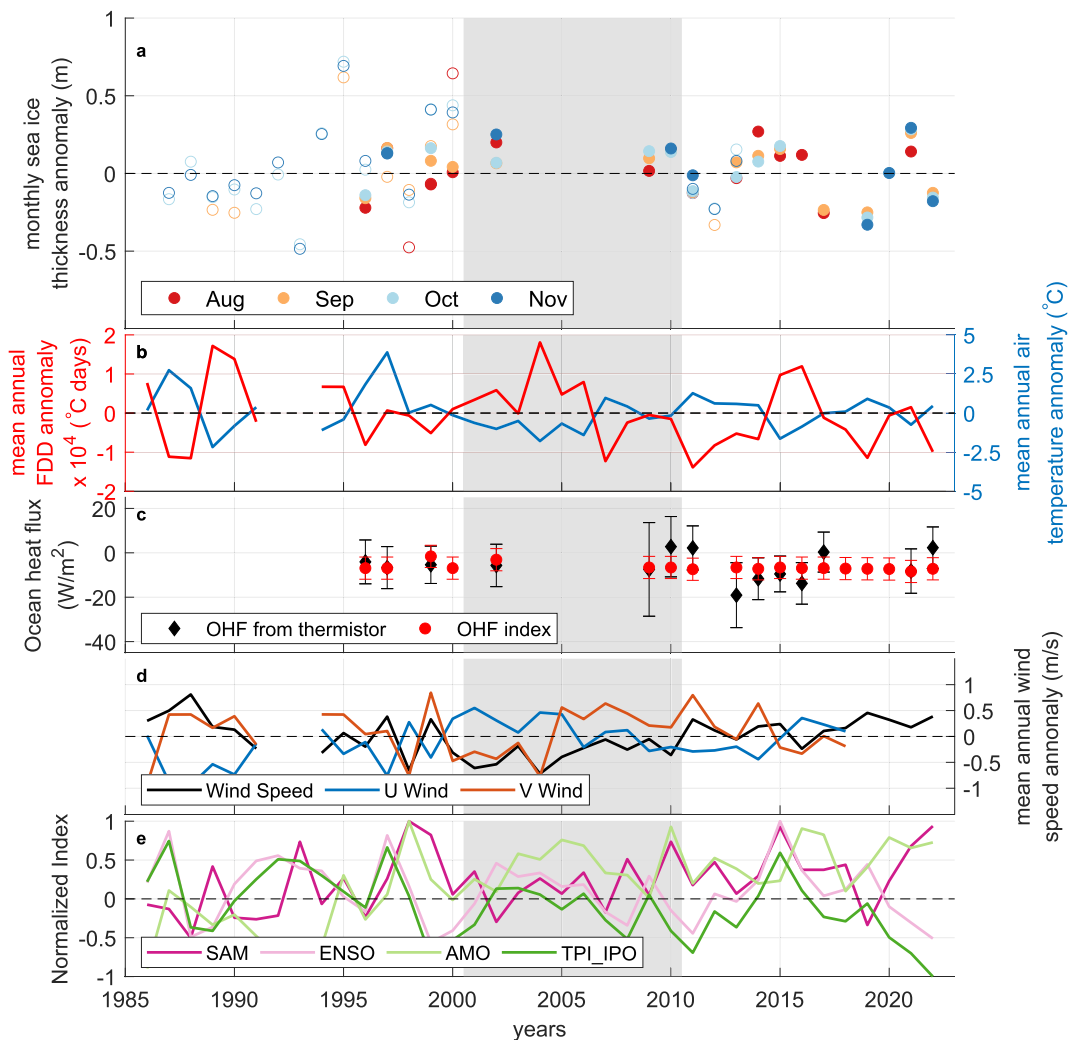


Figure 6. Time series of thicknesses and drivers. Grayed-out area shows time of widespread multi-year ice in the sound due to icebergs. (a) Monthly mean thickness anomaly of first-year ice. Open circles show data from Kim et al. (2018), filled circles show data from our sea-ice monitoring stations (SIMS), colors show month of observation. (b) Mean annual anomaly of freezing degree day (FDD; red) and air temperature (blue), measured at Scott Base. (c) Ocean heat flux from SIMS temperatures following (Smith et al., 2012) in black and ocean heat flux index from Langhorne et al. (2015) in red. (d) Mean annual wind speed anomaly (black), and meridional (southerly, V wind, orange) and zonal components (easterly, U wind, blue), measured at McMurdo Station. (e) Normalized climate indices, Southern Annular Mode (SAM), El-Niño Southern-Oscillation (ENSO) 3.4 Index, Atlantic Multidecadal Oscillation (AMO), Tripole Index of the Interdecadal Pacific Oscillation (TPI_IPO).

Correlations between fast-ice thickness and climate modes are shown in Figure 8. We found no significant correlations with AMO or ENSO. Summer (DJF) IPO was positively correlated with K2018 thicknesses. Winter (JJA) and July IPO were anti-correlated with K2018 thicknesses (but JJA IPO was correlated with October SIMS thicknesses) and May IPO was anti-correlated with the combined and SIMS thicknesses. Autumn and Winter SAMxENSO were anti-correlated with K2018 thicknesses. The only significant correlation between SAM and thickness was for June SAM and November thickness measured by the SIMS, which were anti-correlated.

5. Discussion

This unique data set, containing fast-ice observations over more than 30 years, allowed the first examination of atmospheric drivers of fast-ice thickness in McMurdo Sound over climatological timescales. Out of over 3,000

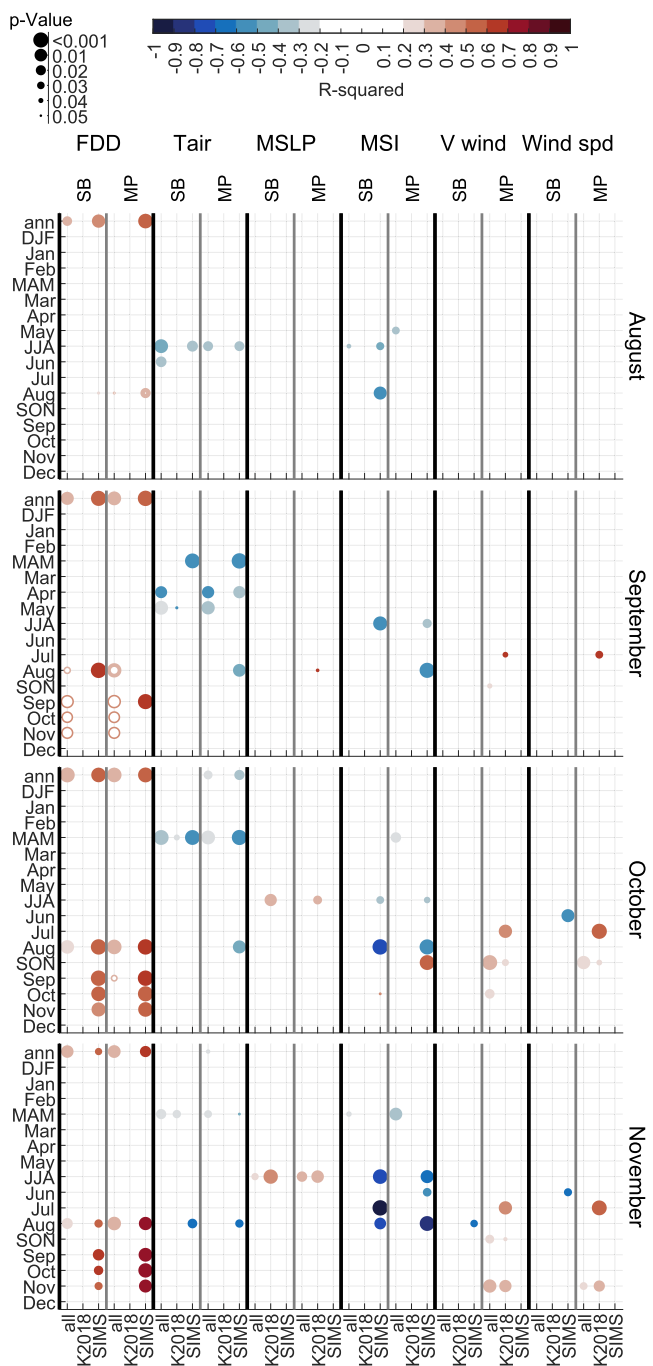


Figure 7. Correlations between fast-ice thickness and meteorological observations from Scott Base (SB), and Marble Point (MP). “All,” “K2018,” and “SIMS” refer to thickness data from all observations, the observations at the sea-ice runway from Kim et al. (2018), and the observations from our sea-ice monitoring stations, respectively. FDD = Freezing Degree Days since start of the year (filled circles) and since the date of fast-ice formation (open circles), MSI = Modified Storm Index, MSLP = pressure at mean sea level, Tair = air temperature, V wind = the meridional wind component, Wind spd = the directionless wind speed. The sign of r^2 is the slope of the fit (negative means anti-correlation, positive means correlation). The size of the circle is proportional to the p -value, large circles are more significant. While correlations have been found among all entries, only correlations with an r^2 value over 0.2 and a p -value below 0.05 are shown. The number of fast-ice thickness observations for each month are shown in Table 2.

tested combinations, among physically reasonable drivers of ice thickness, we presented those driver–response pairings that were significant to $p < 0.05$ and that had an r^2 value larger than 0.2.

We will first discuss why we feel justified in having excluded spatial location within the study site as a factor affecting fast-ice thickness in our data set. We will then discuss the results of the investigation of our two main aims (a) identifying the main meteorological drivers of interannual fast-ice thickness variability; and (b) whether larger scale influences, such as climate modes, have a significant effect.

As described in the Introduction, we examined meteorological observations that either have an influence on atmospheric heat flux or fast-ice persistence, or are used to calculate a derived variable, as with mean sea level pressure and the MSI. We examined this for all three meteorological stations in McMurdo Sound that had sufficient coverage (see Table S2 in Supporting Information S1) since, especially in the case of wind, the location of the station will bring certain biases with it. In addition, we looked at all available thickness data as well as the K2018 and SIMS data separately. Correlation coefficients were higher for shorter time series. No variable was significantly correlated with thickness for both the K2018 and SIMS subsets of our data, and the entire data set.

We will discuss the correlations between thickness and forcings linked to atmospheric heat flux (air temperature and FDD), and then examine dynamic effects via the MSI and freeze-up date. Finally, we will examine the effect of selected climate modes on fast-ice thickness, before ending with a look at possible future research.

Further points to keep in mind throughout the discussion of the results are that: (a) the time series studied is still quite short, even though it exceeds the 30 years length defined for climate means by the WMO (World Meteorological Organization (WMO), 1989; World Meteorological Organization (WMO), 2007); (b) the effect of the large icebergs on McMurdo Sound in the middle of our observation period was likely strong; and (c) we had little information on temporal variability of oceanographic conditions covering our study period, which precluded investigation of this important driver for fast-ice growth in the sound. Regarding (a), Murphy et al. (2014) have found that fast-ice duration, formation, and breakup from 1903 to 2008 shows variability with periods between 2 and 20 years, and the dominant periods of variability changes over the record. To our knowledge, Murphy et al. (2014) have presented the longest record of fast-ice conditions in Antarctica. Whether trends in variables, or correlations between fast-ice conditions and drivers (such as SAM and ENSO), were significant depended on the subset of data chosen (Murphy et al., 2014). This illustrates that care needs to be taken when examining time series, and our time series may still be too short to reveal robust trends and correlations that operate on multi-decadal time periods. Regarding (b), the sensitivity of local fast-ice conditions to grounded icebergs has been well documented (e.g., Brunt et al., 2006; Fraser et al., 2012, 2021; Kim et al., 2018; Massom et al., 2001), and remains a significant barrier to forecasting fast-ice conditions in the Southern Ocean (Fraser et al., 2023). We attempted to mitigate the effect of the icebergs on our study by excluding all observations we knew to be on multi-year ice. However, first-year ice observed during the iceberg years may have still experienced altered forcing, for example, due to altered ocean circulation (Robinson & Williams, 2012). Regarding (c), we noted above that winter ocean temperature has been relatively stable over the past decades (Langhorne et al., 2015), justifying the use of time-averaged ocean heat flux index in the sound and our assumption that the variability in ocean temperature is small.

The location of the measurements within the study area did not have a significant impact on either freeze-up date (Figures 2a and 4a) or on ocean heat flux (Figures 4b and 5). Additionally, the variability in fast-ice thickness at the SIMS sites was similar or lower than that at the K2018 site. This argues that temporally varying atmospheric and oceanic drivers are more important for explaining the variation in thickness in the SIMS data than location within the small study area. The lack of correlation between the mid to late winter ocean heat flux calculated from sea-ice temperature gradients and thickness means that ocean temperature is unlikely to be a major driver of interannual variability in our fast-ice thickness measurements. Influences on fast-ice growth in the early parts of winter are not resolved in our heat-flux calculations. Note that the conductive, latent and ocean heat fluxes are for time periods in which the thermistor probes were deployed, after the ice had reached a thickness of over 1 m and probably after the ocean heat flux in eastern McMurdo Sound had turned negative (Leonard et al., 2006; Mahoney et al., 2011; Robinson et al., 2014). Thus, they reflect the conditions under which ice grew in late winter. The lack of correlation between thickness and heat fluxes in the later part of the growth season points to the importance of the early growth season on fast-ice thickness. It additionally points toward the influence of combinations of individual atmospheric and oceanic drivers, not total heat flux, during the August to November period of observations. These drivers will be examined below.

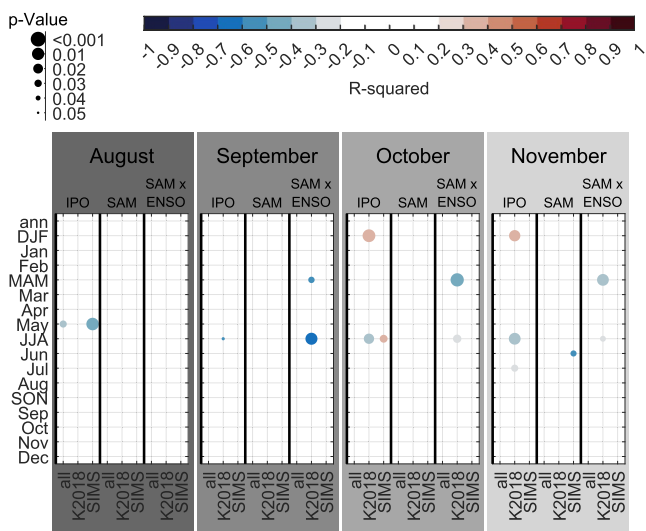


Figure 8. “All,” “K2018,” and “SIMS” refer to thickness data from all observations, the runway observations from Kim et al. (2018), and the observations from our sea-ice monitoring stations, respectively. AMO = Atlantic Multidecadal Oscillation, ENSO = El-Niño Southern Oscillation, IPO = Interdecadal Pacific Oscillation, SAM = Southern Annular Mode. The sign of r^2 is the slope of the fit (negative means anti-correlation, positive means correlation). The size of the circle is proportional to the p -value, large circles are more significant. While correlations have been found among all entries, only correlations with an r^2 value over 0.2 and a p -value below 0.05 are shown.

Importantly, we found no temporal trend in fast-ice thickness for our data set. A previous study by Ainley et al. (2015), that argued that fast-ice thickness in McMurdo Sound had decreased since the 1970s, could not be confirmed by Kim et al. (2018) or our own study. The Ainley et al. (2015) study based their conclusion on the reduced time the icebreaker needed to travel from the fast-ice edge to McMurdo Station, without taking into account technological advances that may have made icebreaking more effective.

5.1. Date of Fast-Ice Formation

An unfortunate drawback to our study is that we did not have regular and precise recordings of freeze-up date for the fast ice in the sound, or even just at the location of the measurements sites. We attempted to extend the excellent time series provided by Fraser and Massom (2020), but were only successful for 2 years in the late 1990s. The need for better and continuous observations of the fast-ice advance and retreat in McMurdo Sound has been known for a long time (Heine, 1963; Prebble, 1968). When presenting a compilation on break out event data from 1902 to 1916, and 1956–1962, Heine (1963) had noted that the position of the southernmost edge of summer fast-ice break out had been recorded photographically since 1958. We do, however, not have knowledge of, or access to, any such records. Heine (1963) had also noted that long-term observations, as well as a predictive capability for break-out events and limits, would be a great advantage to on-ice operations which is confirmed by Falconer and Pyne (2004). Although we and Leonard et al. (2021) find indications for storm-induced winter break out, the event driven nature of fast-ice persistence and break up remain an open field of study.

5.2. Correlations Between Fast-Ice Thickness and Air Temperature

As mentioned in Richter et al. (2022), McMurdo Sound fast-ice growth is unusual compared to fast ice that grows without the influence of ocean supercooling. Instead of the growth rate decreasing with increasing fast-ice thickness (e.g., Maykut, 1986), once platelet ice is incorporated into the sea ice, the sea ice maintains an almost constant or even increasing overall growth rate. This was still true if we examine thickness against FDD (instead of time) as done in Figure 4, and has been attributed to an increasing contribution of ocean heat flux to growth as the fast-ice grows thicker (e.g., Gough et al., 2012; Purdie et al., 2006; Smith et al., 2012; Wongpan et al., 2021). As expected, fast-ice thickness was anti-correlated with air temperature and correlated with FDD (Figure 7). The notable exception was the lack of such a correlation for the K2018 data presented in Kim et al. (2018) confirming their earlier findings. Since the K2018 site was kept snow free over the months studied here, we would have expected a stronger influence of air temperature on thickness for the K2018 data. One possible explanation could be that interannual variation in fast-ice thickness at the K2018 site was determined by the growth rate of the ice before late August/early September when snow was cleared and measurements began. The absence of a correlation between air temperature and fast-ice thickness at the K2018 site may also be linked to the absence of a trend in air temperature over the period the K2018 data was collected (1986–2013), with increasing air temperatures only observed for the SIMS period (1996–2022; see Figure S1 in Supporting Information S1). This was opposite to the global mean air-temperature trend, which saw slower warming since roughly 2000 (e.g., Fyfe et al., 2016) linked to a change in phase of the IPO (e.g., Dai et al., 2015).

Calculating FDD since freeze up, as opposed to FDD since start of the year, did not improve the explanatory power of this variable for the data collected at the SIMS sites. For the combined data, however, FDD since freeze up was significantly correlated with fast-ice thickness, whereas FDD since start of the year was mostly not. Fast-ice breakout in McMurdo Sound occurs in January or February, close to the start of the year, and there is relatively little time for FDD since start of the year to influence the previous season's fast ice before it breaks out. Thus, FDD since start of the year mainly influences any pre-conditioning of the ocean and the new ice forming in the sound. We were not able to determine why calculating FDD since freeze up was able to explain the combined thicknesses better than FDD since start of the year or air temperature. A possible contributing factor could be that freeze-up

dates were only available for data that had been collected since the mid 1990s, thus FDD since freeze up was over a much shorter time period. It may be that FDD only significantly influenced thickness variability from the mid 1990s (roughly the time covered by the SIMS data) and not for the preceding decade.

Contrary to expectations, fast-ice thickness in McMurdo Sound appears not to be dominated by air temperature, with temperature just one of several drivers of similar importance.

5.3. Correlations of Fast-Ice Thickness With MSI, Wind, and Freeze-Up Date

Figure 7 shows a clear change in the effect of storminess, as expressed by the MSI, and wind speed on fast-ice thickness in winter. The MSI was anti-correlated with thickness prior to September and correlated with thickness for spring (SON). Wind speed was anti-correlated with thickness prior to July and correlated for months after July.

Greater storminess from autumn (MAM) to August, as expressed by the MSI, was associated with thinner ice, most strongly for the SIMS data. Prior to May, greater storminess may delay fast-ice formation, thus leading to thinner ice. After May the anti-correlation between MSI and fast-ice thickness may reflect the impact of warmer air advected during storms. However, this effect was not always expressed in the monthly averaged temperatures, for example, while the winter (JJA) MSI from Scott Base observations was anti-correlated with thickness, the winter (JJA) Scott Base temperature was not. The correlation between October fast-ice thickness from the SIMS and the MSI was possibly due to higher atmospheric heat flux due to higher wind speeds. Some confirmation for this theory was given by the positive correlations of fast-ice thickness with winter and spring wind speed as well as meridional (southerly) wind. If higher wind speeds remove snow, leading to greater atmospheric heat flux, this may have also contributed. Unfortunately, we did not have sufficient snow data available to test this hypothesis.

Higher wind speeds during the sea-ice growth season (mostly from the southerly wind component) were correlated with thicker fast ice (Figure 7). We would expect cold winds from the continent to come from the south, and the V component of the wind was significantly anti-correlated with temperature for JJA and SON (not shown), so this could be connected to higher atmospheric heat loss through cold winds. Conversely, wind speed was correlated with air temperature for winter months (not shown). Thus, the effect of wind speed on fast-ice thickness was most probably due to the higher wind speeds themselves causing greater atmospheric heat flux, or, alternatively, due to wind driven snow removal. Again, it is possible that monthly averages did not adequately capture storm events. The anti-correlation between winter wind speed and fast-ice thickness reported in Heil (2006) was only evident for a subset of our data.

A higher MSI in autumn (MAM) and especially April was associated with later fast-ice formation at our sites, as described in Brunt et al. (2006); Leonard et al. (2021). However, the correlations between MSI and freeze-up were weak, and a linear regression between monthly averages is unlikely to capture the event-driven nature of the break-out process during the fast-ice growth season in McMurdo Sound (Leonard et al., 2021). The event-driven nature of fast-ice persistence and break up remain an open field of study.

5.4. Correlations Between Fast-Ice Thickness and Climate Modes

Due to a lack of studies on interactions between climate modes and fast-ice or sea-ice thickness, we will discuss our findings with the available literature on more general climate mode–sea ice interactions. We note that a process that causes greater pack ice concentration or extent does not necessarily also cause greater sea-ice or fast-ice thickness.

Since 2019, the phases of AMO and SAM have become increasingly positive and the phases of ENSO and IPO have become increasingly negative (Figure 6e). This strong opposing behavior is unprecedented over our 1986–2022 time series and has been linked to a deeper Amundsen Sea Low (Chung et al., 2022; Clem & Fogt, 2013; Meehl et al., 2016) and stronger southerly wind in the western Ross Sea (Coggins & McDonald, 2015). Strong, frequent southerly winds have been linked to the frequent wintertime break out of fast ice in McMurdo Sound in 2019 (Leonard et al., 2021) and may have been responsible for the same pattern in 2022. Further work is necessary to establish what drove the 2019 and 2022 fast-ice persistence and thickness and if they are related to changes in large scale climate modes.

The correlations between fast-ice thickness and summer (DJF) IPO (Figure 8), and a lack of such correlations in the atmospheric variables (Figure 7), point toward a possible preconditioning in the ocean as seen by Murphy

et al. (1995, 2014). This merits future investigation. A more negative IPO has been linked to a deeper Amundsen Sea Low (Chung et al., 2022; Meehl et al., 2016) and this in turn has been linked to stronger southerly winds in the western Ross Sea (Coggins & McDonald, 2015). A more negative wintertime IPO and stronger winter southerly wind was associated with thicker fast ice in our study (Figures 7 and 8). There are indications that the recent strong sea-ice retreat around Antarctica is in part due to the switch to a positive IPO phase around 2015 (Meehl et al., 2019).

Our results show that if SAM and ENSO are in phase (both are negative or both are positive) the fast-ice is thinner (Figure 8). SAM and ENSO in opposing phases, for example, a positive SAM and a negative ENSO, have been shown to have a greater effect on sea ice than ENSO on its own (Clem et al., 2017; Stammerjohn et al., 2008) which appears to hold for fast-ice thickness in our study.

A negative ENSO and a more positive SAM have been linked to lower air temperatures and greater sea-ice concentration in the Ross Sea (Clem et al., 2017). Neither ENSO nor SAM on their own showed strong relationships with thickness in our study. In general, correlations between climate modes and fast-ice thickness were absent or weak. This may be due to the relatively short timeseries compared to multi-decadal variability in modes. It remains an open question if and how large scale climate modes influence both pack ice generally and fast ice in McMurdo Sound specifically.

5.5. Future Research

This study illustrates the value of dedicated long-term observational time series to better understand fast-ice growth, and illuminates some of the gaps in current observations that would be of benefit to fill. Given its importance to Antarctic field operations, ice-shelf stability, ice-shelf–cavity–sea-ice–ocean interactions, and the local biosphere, there is a need to improve our knowledge of both year-to-year and long-term changes in fast ice. The SIMS has the advantage over the manual measurements at the sea-ice runway (K2018) that the sea-ice thickness is recorded automatically, continuously, and with minimal disturbance to the ice. The disadvantage of the SIMS data in McMurdo Sound is the varying deployment locations. In the past, these were driven by the needs of science projects that differed from year-to-year. However, it would be an asset to select a dedicated and easily accessible site, situated on stable ice even in years with comparatively little fast-ice cover in the sound. SIMS without acoustic sensors are relatively inexpensive (Jackson et al., 2013), and an argument could be made for having more than one station deployed. Especially in years in which specific scientific inquiries make deploying a SIMS at a location other than the long-term observing site desirable. SIMS which have the capacity to measure snow and SIPL thickness through heating elements would provide the additional advantage of gaining insight to the ocean component of fast-ice growth in supercooled water (e.g., Hoppmann et al., 2015). In addition, a long-term commitment to an oceanographic mooring in the sound, co-located with the SIMS if possible, would allow this unknown component to be studied more fully and give insights to long-term variability in the cavity circulation. With warming ocean temperatures making ice shelf cavities ever more vulnerable, we might be losing the opportunity to gather baseline data on the McMurdo Ice Shelf in a “healthy” state.

A knowledge of the connection between drivers and fast-ice thickness allows projections on longer scales. This has been attempted by Fraser et al. (2023) using the air temperature–fast-ice thickness relationship from Heil (2006) and projected air temperature changes from CMIP6 models (Fraser et al., 2023) have estimated a thickness change in fast ice of -0.14 m by 2100. In addition to air temperature increases, Fraser et al. (2023) have also seen an Antarctic-wide decrease in southerly and easterly winds in their model ensemble. According to our research, a decrease in wind speed would lead to an additional decrease in fast-ice thickness (Figure 7). However, Fraser et al. (2023) have found a projected increase in southerly winds in autumn and winter in the western Ross Sea. Such a scenario could either lead to thicker ice as in the correlations presented here, or it may lead to thinner ice due to frequent break up during the growth season, and thus delayed fast-ice formation (this study and Leonard et al. (2021)). This demonstrates the need for process studies to better understand physical drivers of fast-ice conditions. Currently, predictive capability for fast ice is severely lacking. This study presents the ground work needed for future process model development, analysis of sub-grid scale variability that needs to be parameterized in models, and validation of regional coupled ocean–atmosphere–sea-ice models.

Our study presents a comprehensive exploratory data analysis of fast-ice thickness and atmospheric drivers in McMurdo Sound. Future research should build on this to include multiple linear regression to study the influence of several drivers together. From there, progress toward more complex modeling of the system can be made.

6. Conclusions

This study is the first time a time series of monthly averaged fast-ice thickness in McMurdo Sound, spanning more than 30 years, has been connected to atmospheric drivers. We found no long-term trend in fast-ice thickness in McMurdo Sound in our data. There was no dominant driver of the interannual variability of fast-ice thickness. Instead, thickness was found to be significantly correlated to a range of meteorological observations. We presented the drivers (out of a total of ~3,000 tested physically plausible combinations) that have the greatest influence on fast-ice thickness. The key influences on fast-ice thickness were freezing degree day (FDD), air temperature (Tair), and the MSI, explaining the highest percentage of variance in the fast-ice thickness. Specifically, lower air temperatures, a higher number of freezing degree days, higher mean sea level pressure, a lower MSI, and higher (southerly) wind speeds are connected to thicker fast ice. This is similar to the results from Heil (2006), who has found that greater fast-ice thickness near Davis Station is associated with lower air temperatures and lower storminess. The lack of significant correlation between thickness and late winter heat fluxes indicates that interannual variability in fast-ice thickness may be primarily influenced by conditions during initial fast-ice formation and the early growth season. Efforts should be made to capture this time period in routine observations.

While individual climate modes showed few and weak correlations with fast-ice thickness, if ENSO and SAM are in phase, fast ice is thinner (Figure 8). In general, climate modes influenced the fast ice on seasonal timescales, whereas the meteorological observations were correlated with fast-ice thickness on both monthly and seasonal timescales. This finding confirms those of Murphy et al. (2014) that different drivers act on different timescales. Consequently, it is necessary to study multi-decadal time series to fully resolve dominant drivers that may vary on interannual to decadal timescales. In addition to examining possible pathways that modulate fast-ice thickness in McMurdo Sound, this study gives a baseline for the range of fast-ice conditions, providing context for any future extremes that may be observed. There remains a need for an event-based analysis, especially around extreme events driving winter fast-ice break up and persistence.

Acronyms

AMO	Atlantic Multidecadal Oscillation
ANOVA	Analysis of variance
ASF	Alaska Satellite Facility
doy	Day of year (Julian day)
ENSO	El-Niño-Southern Oscillation
ESA	European Space Agency
FDD	Freezing degree days
IPO	Interdecadal Pacific Oscillation
ISW	Ice shelf water
K2018	Kim et al. (2018)
MSI	Modified storm index
SAM	Southern Annular Mode
SAMxENSO	Normalized SAM index multiplied with the normalized ENSO index
SIMS	Sea-ice monitoring station
SIPL	Sub-ice platelet layer
Tair	Air temperature

Data Availability Statement

Thermistor data collected in McMurdo Sound in 2002 and 2003 were part of the project “Measurements and Improved Parameterization of the Thermal Conductivity and Heat Flow through First-Year Sea Ice,” OPP-0126007*. Data collected in 2009, 2010, and 2013 are available at the data repository PANGAEA (Gough et al., 2017a, 2017b; Smith, Leonard, Langhorne, et al., 2017; Smith, Leonard, Trodahl, et al., 2017). The thermistor data in McMurdo Sound collected after 2009 were collected with the following funding and logistics support: IRL Subcontract to the University of Otago (2010, 2011); University of Otago Research Grants (2010, 2011, 2014, 2015 (Event Manager: Inga Smith)); NIWA subcontract to University of Otago, “Antarctic and High Latitude Climate” (2013–2018); Contribution from MBIE-funded project “Antarctic sea ice thickness: harbinger of change in the Southern Ocean” (2013 (PIs: Pat Langhorne and Wolfgang Rack)); Contribution from MBIE-funded Curious Minds public engagement project “Far from Frozen” (2016, (leader: Craig Grant, Otago Museum)); US Fulbright Scholar Award (Cecilia Bitz, 2013); NZARI (2015 (PIs: Pat Langhorne and Craig Stevens), 2017, 2018 (PI: Greg Leonard)) Deep South National Science Challenge project TOPIMASI (2016–2018 (PI: Pat Langhorne)); Antarctic Science Platform (ASP) Project 4 (Sea ice and carbon cycles) (University of Otago sub-contract 19424 from VUW’s ASP Project 4 contract with Antarctica New Zealand through MBIE SSIF Programmes Investment contract number ANTA1801.) (2019–2022 (Event Manager: Greg Leonard)); Marsden Fund project “Supercooling measurements under ice shelves” (2020 (PI: Inga Smith)) and will be made available through PANGAEA. The monthly mean thickness values calculated from the SIMS data and used in this study are available at <https://doi.org/10.5281/zenodo.8353757> (Richter et al., 2023). The Circum-Antarctic landfast sea ice extent is available at https://data.aad.gov.au/metadata/AAS_4116_Fraser_fastice_circumantarctic (Fraser & Massom, 2020). NIWA’s National Climate Database on the Web (CliFlo) is available at <https://cliflo.niwa.co.nz/>, it was last accessed August 2022. The Marble Point weather station data is available at <http://amrc.ssec.wisc.edu/data/ftp/pub/aws/antrdr/>. We acknowledge Dr Gareth Marshall for the SAM data (Marshall, 2003), and the International Research Institute for Climate Prediction for the Niño 3.4 index data. SAM data downloaded June 2021 from <http://www.nerc-bas.ac.uk/icd/gjma/sam.html>. The Niño 3.4 index was accessed in June 2021 through <http://iridl.ldeo.columbia.edu/SOURCES/Indices/.nino./EXTENDED.NINO34/datafiles.html>. The unsmoothed, detrended AMO from the Kaplan SST V2 data set (Enfield et al., 2001) was calculated at NOAA PSL1 and is available at <http://www.psl.noaa.gov/data/timeseries/AMO/>, last accessed June 2021. The unfiltered IPO Tripole Index of Henley et al. (2015) based on ERSST V5 was created at NOAA PSL and is available at <https://psl.noaa.gov/data/timeseries/IPOTPI/>, last accessed June 2021.

Acknowledgments

We thank Matt Lazarra, David Mikolajczyk, and Taylor Norton for assistance in accessing the Marble Point weather data. The authors appreciate the support of the University of Wisconsin–Madison Automatic Weather Station Program for the Marble Point data set, data display, and information, NSF Grant 1924730. We acknowledge Joe Trodahl and Myles Thayer for work on designing and building the VUW and University of Otago design thermistor probes used in this study, and Peter Stroud, the late Richard Sparrow, and Jim Woods for their assistance. Scott Base winter staff carried out deployment and maintenance of the SIMS. Wolfgang Rack, Adrian McDonald, and James Renwick are acknowledged for helpful discussions on McMurdo Sound Meteorology and fast ice. Jeff Scannello is thanked for his insights into the sea ice runway data collection. MER was funded by a University of Otago Doctoral Scholarship, an Antarctica New Zealand Sir Robin Irvine Doctoral Scholarship, and by the High Latitude and Antarctic Climate project (CAOA2203: NIWA subcontract to the University of Otago). Te Pūnaha Matatini provided MER with financial support to enable this research to be presented and discussed with international colleagues. We acknowledge the funding of the Antarctic Science Platform for the 2020 and 2021 SIMS deployments.

References

Ainley, D. G., Larue, M. A., Stirling, I., Stammerjohn, S., & Siniiff, D. B. (2015). An apparent population decrease, or change in distribution, of Weddell seals along the Victoria Land coast. *Marine Mammal Science*, 31(4), 1338–1361. <https://doi.org/10.1111/mms.12220>

Arndt, S., Hoppmann, M., Schmithüsen, H., Fraser, A. D., & Nicolaus, M. (2020). Seasonal and interannual variability of landfast sea ice in Atka Bay, Weddell Sea, Antarctica. *The Cryosphere*, 14(9), 2775–2793. <https://doi.org/10.5194/tc-14-2775-2020>

Assmann, K. M. (2004). *The effect of McMurdo Sound topography on water mass exchange across the Ross Ice Shelf front* (Vol. 15). Annual report of the Filchner-Ronne Ice Shelf Program (FRISP).

Baba, K., & Renwick, J. (2017). Aspects of intraseasonal variability of Antarctic sea ice in austral winter related to ENSO and SAM events. *Journal of Glaciology*, 63(241), 838–846. <https://doi.org/10.1017/jog.2017.49>

Ball, F. K. (1956). The theory of strong katabatic winds. *Australian Journal of Physics*, 9(3), 373–386. <https://doi.org/10.1071/PH560373>

Bitz, C. M., & Lipscomb, W. H. (1999). An energy-conserving thermodynamic model of sea ice. *Journal of Geophysical Research*, 104(C7), 15669–15677. <https://doi.org/10.1029/1999JC00100>

Brett, G. M., Irvin, A., Rack, W., Haas, C., Langhorne, P. J., & Leonard, G. H. (2020). Variability in the distribution of fast ice and the sub-ice platelet layer near McMurdo ice shelf. *Journal of Geophysical Research: Oceans*, 125(3), e2019JC015678. <https://doi.org/10.1029/2019je015678>

Brunt, K. M., Sergienko, O., & MacAyeal, D. R. (2006). Observations of unusual fast-ice conditions in the southwest Ross Sea, Antarctica: Preliminary analysis of iceberg and storminess effects. *Annals of Glaciology*, 44, 183–187. <https://doi.org/10.3189/172756406781811754>

Cassano, J. J., Nigro, M. A., & Lazarra, M. A. (2016). Characteristics of the near-surface atmosphere over the Ross Ice Shelf, Antarctica. *Journal of Geophysical Research: Atmospheres*, 121(7), 3339–3362. <https://doi.org/10.1002/2015JD024383>

Chenoli, S. N., Turner, J., & Samah, A. A. (2012). A climatology of strong wind events at McMurdo station, Antarctica. *International Journal of Climatology*, 33(12), 2667–2681. <https://doi.org/10.1002/joc.3617>

Chung, E.-S., Kim, S.-J., Timmermann, A., Ha, K.-J., Lee, S.-K., Stuecker, M. F., et al. (2022). Antarctic sea-ice expansion and Southern Ocean cooling linked to tropical variability. *Nature Climate Change*, 12(5), 461–468. <https://doi.org/10.1038/s41558-022-01339-z>

Clem, K. R., & Fogt, R. L. (2013). Varying roles of ENSO and SAM on the Antarctic Peninsula climate in austral spring. *Journal of Geophysical Research: Atmospheres*, 118(20), 11481–11492. <https://doi.org/10.1002/jgrd.50860>

Clem, K. R., Renwick, J. A., & McGregor, J. (2017). Large-scale forcing of the Amundsen Sea Low and its influence on Sea Ice and west Antarctic temperature. *Journal of Climate*, 30(20), 8405–8424. <https://doi.org/10.1175/jcli-d-16-0891.1>

Coggins, J. H. J., & McDonald, A. J. (2015). The influence of the Amundsen Sea Low on the winds in the Ross Sea and surroundings: Insights from a synoptic climatology. *Journal of Geophysical Research: Atmospheres*, 120(6), 2167–2189. <https://doi.org/10.1002/2014jd022830>

Coggins, J. H. J., McDonald, A. J., & Jolly, B. (2013). Synoptic climatology of the Ross Ice Shelf and Ross Sea region of Antarctica: *k*-means clustering and validation. *International Journal of Climatology*, 34(7), 2330–2348. <https://doi.org/10.1002/joc.3842>

Crocker, G. B., & Wadhams, P. (1989). Breakup of Antarctic fast ice. *Cold Regions Science and Technology*, 17(1), 61–76. [https://doi.org/10.1016/s0165-232x\(89\)80016-3](https://doi.org/10.1016/s0165-232x(89)80016-3)

Dai, A., Fyfe, J. C., Xie, S.-P., & Dai, X. (2015). Decadal modulation of global surface temperature by internal climate variability. *Nature Climate Change*, 5(6), 555–559. <https://doi.org/10.1038/nclimate2605>

Dale, E. (2020). *Interactions between changing weather patterns and the Antarctic cryosphere in the Ross Sea region* (unpublished PhD thesis). Environmental Research Group Department of Physical and Chemical Sciences, University of Canterbury.

Dempsey, D. E., Langhorne, P. J., Robinson, N. J., Williams, M. J. M., Haskell, T. G., & Frew, R. D. (2010). Observation and modeling of platelet ice fabric in McMurdo Sound, Antarctica. *Journal of Geophysical Research*, 115(C1). <https://doi.org/10.1029/2008jc005264>

Enfield, D. B., Mestas-Nuñez, A. M., & Trimble, P. J. (2001). The Atlantic Multidecadal Oscillation and its relation to rainfall and river flows in the continental U.S. *Geophysical Research Letters*, 28(10), 2077–2080. <https://doi.org/10.1029/2000gl1012745>

Falconer, T. R., & Pyne, A. R. (2004). Ice breakout history in southern McMurdo Sound, Antarctica (1988–2002). In *Antarctic data series*. Antarctic Research Centre: Victoria University of Wellington.

Fraser, A. D., & Massom, R. (2020). Circum-Antarctic landfast sea ice extent, 2000–2018. *Australian Antarctic Data Centre*. <https://doi.org/10.26179/5D267D1CEB60C>

Fraser, A. D., Massom, R. A., Handcock, M. S., Reid, P., Ohshima, K. I., Raphael, M. N., et al. (2021). Eighteen-year record of circum-Antarctic landfast-sea-ice distribution allows detailed baseline characterisation and reveals trends and variability. *The Cryosphere*, 15(11), 5061–5077. <https://doi.org/10.5194/tc-15-5061-2021>

Fraser, A. D., Massom, R. A., Michael, K. J., Galton-Fenzi, B. K., & Lieser, J. L. (2012). East Antarctic landfast sea ice distribution and variability, 2000–08. *Journal of Climate*, 25(4), 1137–1156. <https://doi.org/10.1175/jcli-d-10-05032.1>

Fraser, A. D., Wongpan, P., Langhorne, P. J., Klekociuk, A. R., Kusahara, K., Lannuzel, D., et al. (2023). Antarctic landfast Sea Ice: A review of its physics, biogeochemistry and ecology. *Reviews of Geophysics*, 61(2). <https://doi.org/10.1029/2022rg000770>

Fyfe, J. C., Meehl, G. A., England, M. H., Mann, M. E., Santer, B. D., Flato, G. M., et al. (2016). Making sense of the early-2000s warming slowdown. *Nature Climate Change*, 6(3), 224–228. <https://doi.org/10.1038/nclimate2938>

Gelman, A., & Hill, J. (2007). *Data analysis using regression and multilevel/hierarchical models*. Cambridge University Press. <https://doi.org/10.1017/CBO9780511790942>

Gough, A. J. (2012). *Sea ice near an ice shelf* (unpublished Ph.D. thesis). University of Otago.

Gough, A. J., Mahoney, A. R., Langhorne, P. J., Williams, M. J. M., Robinson, N. J., & Haskell, T. G. (2012). Signatures of supercooling: McMurdo Sound platelet ice. *Journal of Glaciology*, 58(207), 38–50. <https://doi.org/10.3189/2012jog10j218>

Gough, A. J., Mahoney, A. R., Langhorne, P. J., Williams, M. J. M., Stevens, C. L., & Haskell, T. G. (2017a). *Sea ice temperature profiles from McMurdo Sound, Antarctica in 2009 from temperature string 2009A (Tanker Channel Site)*. PANGAEA - Data Publisher for Earth & Environmental Science. <https://doi.org/10.1594/PANGAEA.880162>

Gough, A. J., Mahoney, A. R., Langhorne, P. J., Williams, M. J. M., Stevens, C. L., & Haskell, T. G. (2017b). *Sea ice temperature profiles from McMurdo Sound, Antarctica in 2009 from temperature string 2009B (Erebus Bay Site)*. PANGAEA - Data Publisher for Earth & Environmental Science. <https://doi.org/10.1594/PANGAEA.880163>

Gow, A. J., Ackley, S. F., Govoni, J. W., & Weeks, W. F. (1998). Physical and structural properties of land-fast Sea Ice in McMurdo Sound, Antarctica. In *Antarctic sea ice: Physical processes, interactions and variability* (pp. 355–374). American Geophysical Union. <https://doi.org/10.1029/AR074p0355>

Haas, C., Langhorne, P. J., Rack, W., Leonard, G. H., Brett, G. M., Price, D., et al. (2021). Airborne mapping of the sub-ice platelet layer under fast ice in McMurdo Sound, Antarctica. *The Cryosphere*, 15(1), 247–264. <https://doi.org/10.5194/tc-15-247-2021>

Heil, P. (2006). Atmospheric conditions and fast ice at Davis, East Antarctica: A case study. *Journal of Geophysical Research*, 111(C5). <https://doi.org/10.1029/2005jc002904>

Heil, P., Allison, I., & Lytle, V. I. (1996). Seasonal and interannual variations of the oceanic heat flux under a landfast Antarctic sea ice cover. *Journal of Geophysical Research*, 101(C11), 25741–25752. <https://doi.org/10.1029/96jc01921>

Heine, A. J. (1963). Ice breakout around the southern end of Ross Island, Antarctica. *New Zealand Journal of Geology and Geophysics*, 6(3), 395–401. <https://doi.org/10.1080/00288306.1963.10422071>

Hellmer, H. H. (2004). Impact of Antarctic ice shelf basal melting on sea ice and deep ocean properties. *Geophysical Research Letters*, 31(L10307). <https://doi.org/10.1029/2004gl019506>

Henley, B. J., Gergis, J., Karoly, D. J., Power, S., Kennedy, J., & Folland, C. K. (2015). A tripole index for the interdecadal Pacific Oscillation. *Climate Dynamics*, 45(11–12), 3077–3090. <https://doi.org/10.1007/s00382-015-2525-1>

Higashi, A., Goodman, D. J., Kawaguchi, S., & Mae, S. (1982). The cause of the breakup of fast ice on March 18, 1980 near Syowa station, East Antarctica. In *Proc. 4th Symposium on Polar Meteorology and Glaciology, National Institute of Polar Research, Tokyo, Japan* (pp. 222–231).

Hobbs, W. R., Massom, R., Stammerjohn, S., Reid, P., Williams, G., & Meier, W. (2016). A review of recent changes in Southern Ocean sea ice, their drivers and forcings. *Global and Planetary Change*, 143, 228–250. <https://doi.org/10.1016/j.gloplacha.2016.06.008>

Hodgson, T. V. (1907). On collecting in Antarctic seas, British National Antarctic Expedition, 1901–1904. In *Zoology and botany* (Vol. 3, pp. 1–10). Trustees of the British Museum.

Hoppmann, M., Nicolaus, M., Hunkeler, P. A., Heil, P., Behrens, L.-K., König-Langlo, G., & Gerdes, R. (2015). Seasonal evolution of an ice-shelf influenced fast-ice regime, derived from an autonomous thermistor chain. *Journal of Geophysical Research: Oceans*, 120(3), 1703–1724. <https://doi.org/10.1002/2014jc010327>

Hoppmann, M., Richter, M. E., Smith, I. J., Jendersie, S., Langhorne, P. J., Thomas, D. N., & Dieckmann, G. S. (2020). Platelet ice, the Southern Ocean's hidden ice: A review. *Annals of Glaciology*, 61(83), 1–28. <https://doi.org/10.1017/aog.2020.54>

Hughes, K. (2013). *Propagation of an ice shelf water plume beneath Sea Ice in McMurdo Sound, Antarctica* (unpublished MSc thesis). University of Otago.

Jackson, K., Wilkinson, J., Maksym, T., Meldrum, D., Beckers, J., Haas, C., & Mackenzie, D. (2013). A novel and low-cost sea ice mass balance buoy. *Journal of Atmospheric and Oceanic Technology*, 30(11), 2676–2688. <https://doi.org/10.1175/jtech-d-13-00058.1>

Jacobs, S. S. (2004). Bottom water production and its links with the thermohaline circulation. *Antarctic Science*, 16(4), 427–437. <https://doi.org/10.1017/s095410200400224x>

Jacobs, S. S., Fairbanks, R. G., & Horibe, Y. G. (1985). Origin and evolution of water masses near the Antarctic continental margin: Evidence from H218O/H216O ratios in seawater. In *Oceanology of the Antarctic continental shelf* (Vol. 43, pp. 59–85). AGU. <https://doi.org/10.1029/AR043p0059>

Kacimi, S., & Kwok, R. (2020). The Antarctic sea ice cover from ICESat-2 and CryoSat-2: Freeboard, snow depth, and ice thickness. *The Cryosphere*, 14(12), 4453–4474. <https://doi.org/10.5194/tc-14-4453-2020>

Kim, S., Saenz, B., Scanniello, J., Daly, K., & Ainley, D. (2018). Local climatology of fast ice in McMurdo Sound, Antarctica. *Antarctic Science*, 30(2), 125–142. <https://doi.org/10.1017/s0954102017000578>

Kurtz, N. T., & Markus, T. (2012). Satellite observations of Antarctic sea ice thickness and volume. *Journal of Geophysical Research*, 117(C8), C08025. <https://doi.org/10.1029/2012jc008141>

Langhorne, P. J., Hughes, K. G., Gough, A. J., Smith, I. J., Williams, M. J. M., Robinson, N. J., et al. (2015). Observed platelet ice distributions in Antarctic sea ice: An index for ocean-ice shelf heat flux. *Geophysical Research Letters*, 42(13), 5442–5451. <https://doi.org/10.1002/2015gl064508>

Leonard, G. H., Langhorne, P. J., Williams, M. J. M., Vennell, R., Purdie, C. R., Dempsey, D. E., et al. (2011). Evolution of supercooling under coastal Antarctic sea ice during winter. *Antarctic Science*, 23(4), 399–409. <https://doi.org/10.1017/S0954102011000265>

Leonard, G. H., Purdie, C. R., Langhorne, P. J., Haskell, T. G., Williams, M. J. M., & Frew, R. D. (2006). Observations of platelet ice growth and oceanographic conditions during the winter of 2003 in McMurdo Sound, Antarctica. *Journal of Geophysical Research*, 111(C4). <https://doi.org/10.1029/2005jc002952>

Leonard, G. H., Turner, K. E., Richter, M. E., Whittaker, M. S., & Smith, I. J. (2021). Brief communication: The anomalous winter 2019 sea-ice conditions in McMurdo Sound, Antarctica. *The Cryosphere*, 15(10), 4999–5006. <https://doi.org/10.5194/tc-15-4999-2021>

Lewis, E. L., & Perkin, R. G. (1985). The winter oceanography of McMurdo Sound, Antarctica. In S. S. Jacobs (Ed.), *Oceanography of the Antarctic continental shelf* (Vol. 43, pp. 145–165). AGU. <https://doi.org/10.1029/AR043p0145>

Mahoney, A. R., Gough, A. J., Langhorne, P. J., Robinson, N. J., Stevens, C. L., Williams, M. M. J., & Haskell, T. G. (2011). The seasonal appearance of ice shelf water in coastal Antarctica and its effect on sea ice growth. *Journal of Geophysical Research*, 116(C11). <https://doi.org/10.1029/2011jc007060>

Marshall, G. J. (2003). Trends in the Southern Annular Mode from observations and reanalyses. *Journal of Climate*, 16(24), 4134–4143. [https://doi.org/10.1175/1520-4442\(2003\)016<4134:fitsam>2.0.co;2](https://doi.org/10.1175/1520-4442(2003)016<4134:fitsam>2.0.co;2)

Massom, R. A., Hill, K. L., Lytle, V. I., Worby, A. P., Paget, M. J., & Allison, I. (2001). Effects of regional fast-ice and iceberg distributions on the behaviour of the Mertz Glacier polynya, East Antarctica. *Annals of Glaciology*, 33, 391–398. <https://doi.org/10.3189/172756401781818518>

Maykut, G. A. (1986). The surface heat and mass balance. In N. Untersteiner (Ed.), *The geophysics of sea ice* (pp. 395–463). Springer US. https://doi.org/10.1007/978-1-4899-5352-0_6

Meehl, G. A., Arblaster, J. M., Bitz, C. M., Chung, C. T. Y., & Teng, H. (2016). Antarctic sea-ice expansion between 2000 and 2014 driven by tropical Pacific decadal climate variability. *Nature Geoscience*, 9(8), 590–595. <https://doi.org/10.1038/ngeo2751>

Meehl, G. A., Arblaster, J. M., Chung, C. T. Y., Holland, M. M., DuVivier, A., Thompson, L., et al. (2019). Sustained ocean changes contributed to sudden Antarctic sea ice retreat in late 2016. *Nature Communications*, 10(1), 14. <https://doi.org/10.1038/s41467-018-07865-9>

Murphy, E. J., Clarke, A., Abram, N. J., & Turner, J. (2014). Variability of sea-ice in the northern Weddell Sea during the 20th century. *Journal of Geophysical Research: Oceans*, 119(7), 4549–4572. <https://doi.org/10.1002/2013jc009511>

Murphy, E. J., Clarke, A., Symon, C., & Priddle, J. (1995). Temporal variation in Antarctic sea-ice: Analysis of a long term fast-ice record from the South Orkney Islands. *Deep Sea Research Part I: Oceanographic Research Papers*, 42(7), 1045–1062. [https://doi.org/10.1016/0967-0637\(95\)00057-d](https://doi.org/10.1016/0967-0637(95)00057-d)

Ono, N. (1967). Specific heat and heat of fusion of sea ice. *Physics of Snow and Ice: Proceedings*, 1(1), 599–610.

Prebble, M. M. (1968). Ice breakout, McMurdo Sound, Antarctica. *New Zealand Journal of Geology and Geophysics*, 11(4), 908–921. <https://doi.org/10.1080/00288306.1968.10420760>

Price, D., Rack, W., Haas, C., Langhorne, P. J., & Marsh, O. (2013). Sea ice freeboard in McMurdo Sound, Antarctica, derived by surface-validated ICESat laser altimeter data. *Journal of Geophysical Research: Oceans*, 118(7), 3634–3650. <https://doi.org/10.1002/jgrc.20266>

Price, D., Rack, W., Langhorne, P., Haas, C., Leonard, G., & Barnsdale, K. (2014). The sub-ice platelet layer and its influence on freeboard to thickness conversion of Antarctic sea ice. *The Cryosphere*, 8(3), 1031–1039. <https://doi.org/10.5194/tc-8-1031-2014>

Pringle, D. J., Eicken, H., Trodahl, H. J., & Backstrom, L. G. E. (2007). Thermal conductivity of landfast Antarctic and Arctic sea ice. *Journal of Geophysical Research*, 112(C4). <https://doi.org/10.1029/2006jc003641>

Pringle, D. J., Trodahl, H. J., & Haskell, T. G. (2006). Direct measurement of sea ice thermal conductivity: No surface reduction. *Journal of Geophysical Research*, 111(C5). <https://doi.org/10.1029/2005jc002990>

Purdie, C., Langhorne, P., Leonard, G., & Haskell, T. (2006). Growth of first-year landfast Antarctic sea ice determined from winter temperature measurements. *Annals of Glaciology*, 44, 170–176. <https://doi.org/10.3189/172756406781811853>

Richter, M. E., Leonard, G. H., Smith, I. J., Langhorne, P. J., Mahoney, A. R., & Parry, M. (2022). Accuracy and precision when deriving sea-ice thickness from thermistor strings: A comparison of methods. *Journal of Glaciology*, 69(276), 1–20. <https://doi.org/10.1017/jog.2022.108>

Richter, M. E., Smith, I. J., Langhorne, P. J., Leonard, G. H., & Gough, A. J. (2023). *Monthly averaged fast-ice thickness in McMurdo Sound from a sea-ice monitoring station*. Zenodo. <https://doi.org/10.5281/zenodo.8353757>

Rienecker, M. M., Suarez, M. J., Gelaro, R., Todling, R., Bacmeister, J., Liu, E., et al. (2011). MERRA: NASA's modern-era retrospective analysis for research and applications. *Journal of Climate*, 24(14), 3624–3648. <https://doi.org/10.1175/JCLI-D-11-00015.1>

Robinson, N. J., & Williams, M. J. M. (2012). Iceberg-induced changes to polynya operation and regional oceanography in the southern Ross Sea, Antarctica, from in situ observations. *Antarctic Science*, 24(5), 514–526. <https://doi.org/10.1017/s0954102012000296>

Robinson, N. J., Williams, M. J. M., Stevens, C. L., Langhorne, P. J., & Haskell, T. G. (2014). Evolution of a supercooled Ice Shelf Water plume with an actively growing subice platelet matrix. *Journal of Geophysical Research: Oceans*, 119(6), 3425–3446. <https://doi.org/10.1002/2013JC009399>

Smith, I. J., Gough, A. J., Langhorne, P. J., Mahoney, A. R., Leonard, G. H., Van Hale, R., et al. (2015). First-year land-fast Antarctic sea ice as an archive of ice shelf meltwater fluxes. *Cold Regions Science and Technology*, 113, 63–70. <https://doi.org/10.1016/j.coldregions.2015.01.007>

Smith, I. J., Langhorne, P. J., Frew, R. D., Vennell, R., & Haskell, T. G. (2012). Sea ice growth rates near ice shelves. *Cold Regions Science and Technology*, 83–84(0), 57–70. <https://doi.org/10.1016/j.coldregions.2012.06.005>

Smith, I. J., Langhorne, P. J., Haskell, T. G., Trodahl, H. J., Frew, R., & Vennell, M. R. (2001). Platelet ice and the land-fast sea ice of McMurdo Sound, Antarctica. *Annals of Glaciology*, 33, 21–27. <https://doi.org/10.3189/172756401781818365>

Smith, I. J., Leonard, G. H., Langhorne, P. J., Trodahl, H. J., Haskell, T. G., Stevens, C. L., et al. (2017). Sea ice temperature profiles from McMurdo Sound, Antarctica in 2013 from a temperature string. *PANGAEA - Data Publisher for Earth & Environmental Science*. <https://doi.org/10.1594/PANGAEA.880165>

Smith, I. J., Leonard, G. H., Trodahl, H. J., Gough, A. J., Langhorne, P. J., & Haskell, T. G. (2017). *Sea ice temperature profiles from McMurdo Sound, Antarctica in 2010 from a temperature string*. PANGAEA - Data Publisher for Earth & Environmental Science. <https://doi.org/10.1594/PANGAEA.880164>

Stammerjohn, S. E., Martinson, D. G., Smith, R. C., Yuan, X., & Rind, D. (2008). Trends in Antarctic annual sea ice retreat and advance and their relation to El Niño–Southern Oscillation and Southern Annular Mode variability. *Journal of Geophysical Research*, 113(C3). <https://doi.org/10.1029/2007jc004269>

Stefan, J. (1891). Ueber die Theorie der Eisbildung, insbesondere über die Eisbildung im Polarmeere. *Annalen der Physik*, 278(2), 269–286. <https://doi.org/10.1002/andp.18912780206>

Trodahl, H. J., McGuinness, M. J., Langhorne, P. J., Collins, K., Pantoja, A. E., Smith, I. J., & Haskell, T. G. (2000). Heat transport in McMurdo Sound first-year fast ice. *Journal of Geophysical Research*, 105(C5), 11347–11358. <https://doi.org/10.1029/1999JC000003>

Wongpan, P., Vancoppenolle, M., Langhorne, P. J., Smith, I. J., Madec, G., Gough, A. J., et al. (2021). Sub-ice platelet layer physics: Insights from a Mushy-layer Sea Ice model. *Journal of Geophysical Research: Oceans*, 126(6), e2019JC015918. <https://doi.org/10.1029/2019JC015918>

World Meteorological Organization (WMO). (1989). *Calculation of monthly and annual 30-year standard normals* (Tech. Rep. No. WMO/TD- No. 341; WCDP- No. 10). World Meteorological Organization (WMO).

World Meteorological Organization (WMO). (2007). *The role of climatological normals in a changing climate* (Tech. Rep. No. WMO/TD- No. 1377; WCDMP- No. 61). World Meteorological Organization (WMO).

Yi, D., Zwally, H. J., & Robbins, J. W. (2011). ICESat observations of seasonal and interannual variations of sea-ice freeboard and estimated thickness in the Weddell Sea, Antarctica (2003–2009). *Annals of Glaciology*, 52(57), 43–51. <https://doi.org/10.3189/172756411795931480>

Yu, L., Zhong, S., Vihma, T., Sui, C., & Sun, B. (2021). Sea ice changes in the Pacific sector of the Southern Ocean in austral autumn closely associated with the negative Polarity of the South Pacific Oscillation. *Geophysical Research Letters*, 48(7), e2021GL092409. <https://doi.org/10.1029/2021gl092409>